BSGF - Earth Sciences Bulletin 2021, 192, 51

https://doi.org/10.1051/bsgf/2021033

Special Issue Orogen lifecycle: learnings and perspectives from Pyrenees, Western Mediterranean and analogues ed. O. Lacombe, S. Tavani, A. Teixell, D. Pedreira and S. Calassou (Guest editors)

Available online at: www.bsgf.fr

OPEN ACCESS

Assessment of the tectonic role of the Triassic evaporites in the North Toulon fold-thrust belt

Vincent Wicker* and Mary Ford

CRPG – Université de Lorraine, 15 rue Notre Dame des Pauvres, 54500 Vandoeuvre-lès-Nancy, France

Received: 1 December 2020 / Accepted: 6 September 2021 / Publishing online: 2 November 2021

Abstract – The eastern Beausset Syncline and Toulon Belt, in the southern France, represents the easternmost remnant of the Pyrenean Apto-Albian Rift System and of the Pyrenean-Provençal orogen (Late Cretaceous-Eocene). Detailed structural and stratigraphic field mapping as well as the integration of published structural and stratigraphic data, are used to reconstruct the Jurassic to Late Cretaceous tectonic evolution of this area. A layered evaporite sequence, composed of a succession of evaporitic units interbedded with more competent lithologies, behaved as the main decoupling horizon and source of diapiric bodies. Structural and lithostratigraphic observations in the Mont Caumes area are interpreted as halokinetic in origin (wedges, flaps, welds, thrust welds, highly localized depocentes). These were controlled by the sinuous Mont Caumes salt wall that grew along the southern flank of the eastern Beausset Syncline and interacted with regional tectonic stresses from Early Jurassic to latest Santonian times. Jurassic and Lower Cretaceous carbonate units thin toward the Mont Caumes salt wall, recording deposition in salt controlled broad synclinal depocentres controlled by early salt mobilization. Inverted relics of Apto-Albian rift depocenters are aligned along the northern margin of the Toulon Belt and the adjacent Bandol Belt to the west. In the Turonian-Coniacian Revest depocenter, stratal thickness variations, progressive unconformities lateral depocentre, and the westward increase in stratal, overturning of a flap on the basin's southern margin all record localized strong asymmetrical growth of the 3D Mont Caumes salt wall. During Pyrenean-Provençal N-S convergence starting in Early Campanian, the salt wall was squeezed and reactivated as a thrust weld. The upper part of the flap was sheared and thrust north over the Beausset Syncline (Mont Caumes imbricate). Further to the west, the Saint-Cyr salt extrusion associated with the Santonian-Muschelkalk unconformity, indicates that the Bandol salt wall extruded at the same time as the main diapiric activity of the Mont Caumes salt wall. Compressional reactivation further extruded the salt body leading to emplacement of the Beausset Klippe onto the Beausset Syncline. The Toulon salt structures can be correlated with other examples of contractional salt structures in the external Alps and Pyrenees.

Keywords: salt tectonics / Toulon Fault Zone / Beausset Syncline / halokinesis / megaflap / Pyrenean-Provençal tectonics

Résumé – Évaluation du rôle tectonique du Trias évaporitique dans les chaînons nord-toulonnais. Le système chevauchant toulonnais, sur le flanc sud du synclinal du Beausset, représente la terminaison du système orogénique pyrénéo-provençal (Crétacé supérieur à Eocène). Un travail de terrain structural et stratigraphique associé à l'intégration de données structurales et stratigraphiques publiées, sont utilisés pour reconstruire l'histoire tectonique du Jurassique au Crétacé supérieur des chaînons nord-toulonnais. Une séquence évaporitique stratifiée, composée d'une succession de niveaux évaporitiques et de niveaux compétents carbonatés, constitue le niveau de décollement majeur qui est à l'origine de mouvements diapiriques. Les structures et les architectures stratigraphiques observées dans le secteur du Mont Caumes sont interprétées comme ayant une origine halocinétique. Les structures salifères observées (séquences halocinétiques, discordances progressives, unités renversées « flap ») se sont développées sur le flanc sud du synclinal du Beausset et sur le flanc nord du diapir du Mont Caumes. L'halocinèse a interagi avec les contraintes déviatoriques régionales au début du Jurassique au Crétacé supérieur (Santonien). Les formations carbonatées Jurassiques et Crétacé inférieurs s'amincissent sur le flanc nord du diapir du Mont

*Corresponding author: vincent.wicker@univ-lorraine.fr

Caumes, enregistrant la croissance de dépocentres contrôlés par le mouvement précoce des évaporites. Les dépocentres Apto-albiens sont alignés le long de la marge nord des chaînons toulonnais et plus à l'ouest au nord de Bandol. La croissance du diapir du Mont Caumes s'enregistre au Turonien et au Coniacien, par la mise en place d'une unité renversée « flap », de discordances progressives et de variations d'épaisseurs remarquables dans les unités Turoniennes et Coniaciennes d'Est en Ouest. Pendant la convergence pyrénéo-provençale, qui débute au Campanien, le diapir du Mont Caumes est détruit et réactivé en chevauchement. De plus, au cours de la convergence, l'unité en série inverse du Mont Caumes, est cisaillée et chevauchée sur le flanc sud du synclinal du Beausset. Plus à l'ouest, l'extrusion de sel de Saint-Cyr, est associée à la discordance du Santonien sur le Muschelkalk, et indique que l'activité du diapir de Bandol est synchrone de celle du diapir du Mont Caumes. La réactivation du diapir de Bandol au cours de la phase pyrénéo-provençale facilite l'extrusion de sel et la mise en place de la klippe du Beausset sur le synclinal du Beausset. Les structures de salifères des chaînons toulonnais peuvent être corrélées avec d'autres exemples de structures salifères compressives dans les Alpes externes ou les Pyrénées.

Mots clés : tectonique salifère / faille de Toulon / synclinal du Beausset / halocinèse / mégaflap / tectonique pyrénéo-provençale

1 Introduction

In salt-rich external orogenic systems, it can be difficult to distinguish deformation related to pre-collisional rifting, halokinetic deformation and compressional deformation, often leading to conflicting interpretations. In particular, the onset of convergence within salt-rich systems can be difficult to identify if the imprint of earlier halokinetic activity is present. While excellent seismic data can enable the construction of high-resolution structural models of offshore structures, the study of field analogues is essential to verify, challenge and further develop these models (*e.g.*, Dardeau and de Granciansky, 1990; Canérot *et al.*, 2005; Graham *et al.*, 2012; Célini *et al.*, 2020). Field documentation of inverted salt structures is, however, extremely challenging because of the difficulty in unambiguously distinguishing and proving the true degree of salt control on deformation in a partly preserved and variably exposed terrain. Added difficulties include: (1) evaporitic lithologies have often been removed through dissolution, deformation or erosion, leaving little or no trace of what once may have been a considerable volume of mobile material, (2) the superposition of several phases of non-cylindrical salt-influenced deformation can produce extremely complex stratal and structural records that (3) may be mistakenly interpreted as recording deviatoric strain. As is now common practice, we here use the term salt to denote evaporitic deposits rich in mobile minerals such as halite, anhydrite and gypsum (Hudec and Jackson, 2007).

Recent regional scale studies have demonstrated the critical role of Triassic salt in the evolution of Pyrenean and Iberian fold belts, the Provence fold and thrust belt, and the southern Subalpine chains from the onset of Triassic rifting to latest Cenozoic shortening (*e.g.*, Canérot *et al.*, 2005; Graham *et al.*, 2012; Saura *et al.*, 2014; Saura *et al.*, 2016; Bestani *et al.*, 2016; Espurt *et al.*, 2019; Vergés *et al.*, 2020; Labaume and Teixell 2020; Ford and Vergés 2020). These new insights have stimulated this investigation into complex structural and stratigraphic geometries in the Toulon area, where allochthonous nappes associated with Triassic evaporites were first recognized by Bertrand in 1887. Bertrand's pioneering interpretations laid the foundations for thin-skinned tectonics. Our aim here is to clarify the role of Triassic salt in the evolution of the key Mont Caumes area and to thus better evaluate the relevance of halokinetic activity for regional tectonic history. The study focuses on the Coastal Inner Units at the southern extremity of the Provence fold and thrust belt (Fig. 1a; Espurt *et al.*, 2019) and, more specifically, on the eastern Toulon Belt, its northern boundary, the Toulon Fault Zone, and the southern Beausset Syncline to the north. The Coastal Inner Units notably preserve the most easterly remnants of Apto-Albian depocentres that formed as part of a major transtensional rift system between Iberia and Europe (Choukroune and Mattauer, 1978; Philip *et al.*, 1987). Reconstructions of this easterly section of the rifted plate margin are challenging due to multiple overprinting, first by N-S Pyrenean-Provençal shortening and later, by backarc opening of the Liguro-Provençal Basin during the Oligo-Miocene that largely destroyed the eastern prolongation of the Pyrenean orogen (Mauffret and Gorini 1996). Pyrenean-Provençal shortening inverted the Coastal Inner Units, translating salt-rich units northward (Bestani *et al.*, 2016; Espurt *et al.*, 2019). While we know that shortening continued until the Eocene, the age of onset of Pyrenean shortening in this critical region is controversial. Complex stratal geometries of early Upper Cretaceous age lie along the northern boundaries of the Coastal Inner Units and may represent either early onset of Pyrenean convergence (Masse and Philip, 1976) and/or important halokinetic deformation (Espurt *et al.*, 2019). The implications for regional reconstructions of each of these interpretations are significant.

The main scientific questions addressed in this paper therefore are: (1) what was the role of salt in the evolution of the Inner Coastal Units of southern Provence?; (2) what are the implications for alpine-cycle convergence in this area?; (3) what is the regional significance of these inverted basins in the context of the Pyrenean orogeny? First, we describe the complex structures and stratal architectures of the eastern Toulon Fault Zone. Then, we reexamine the role of evaporite in the Toulon Fault Zone by reconstructing the geological history of the area. Finally, we discuss the regional significance of our findings for Cretaceous to Cenozoic paleogeographic and tectonic reconstructions.

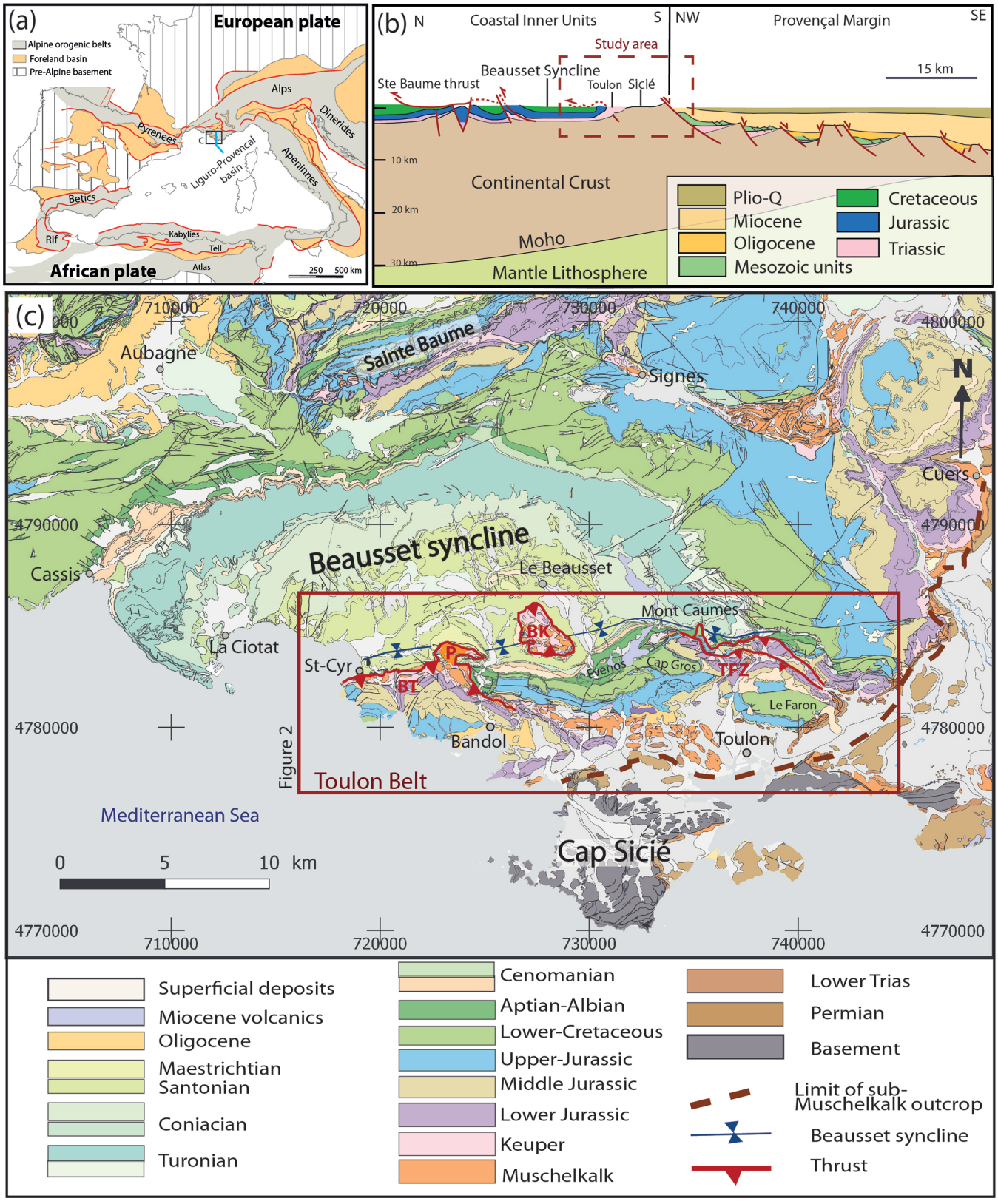

Fig. 1. Geological setting. (a) Map of Alpine orogens of the western Mediterranean region showing the location of the study area (box). The blue trace represents the location of the regional section in b. (b) Simplified regional transect of the onshore eastern Provence fold belt (with study area) and the offshore passive margin of the Oligocene Liguro-Provençal Basin (adapted from Guieu and Roussel, 1990). (c) Geological map of the Beausset Syncline and the Inner Coastal Units of eastern Provence showing the location of Figure 2. Adapted from BRGM maps (Gouvernet *et al.*, 1969). Abbreviations: BT: Bandol Thrust; P: Pibernon Half-Klippe; BK: Beausset Klippe; TFZ: Toulon Fault Zone.

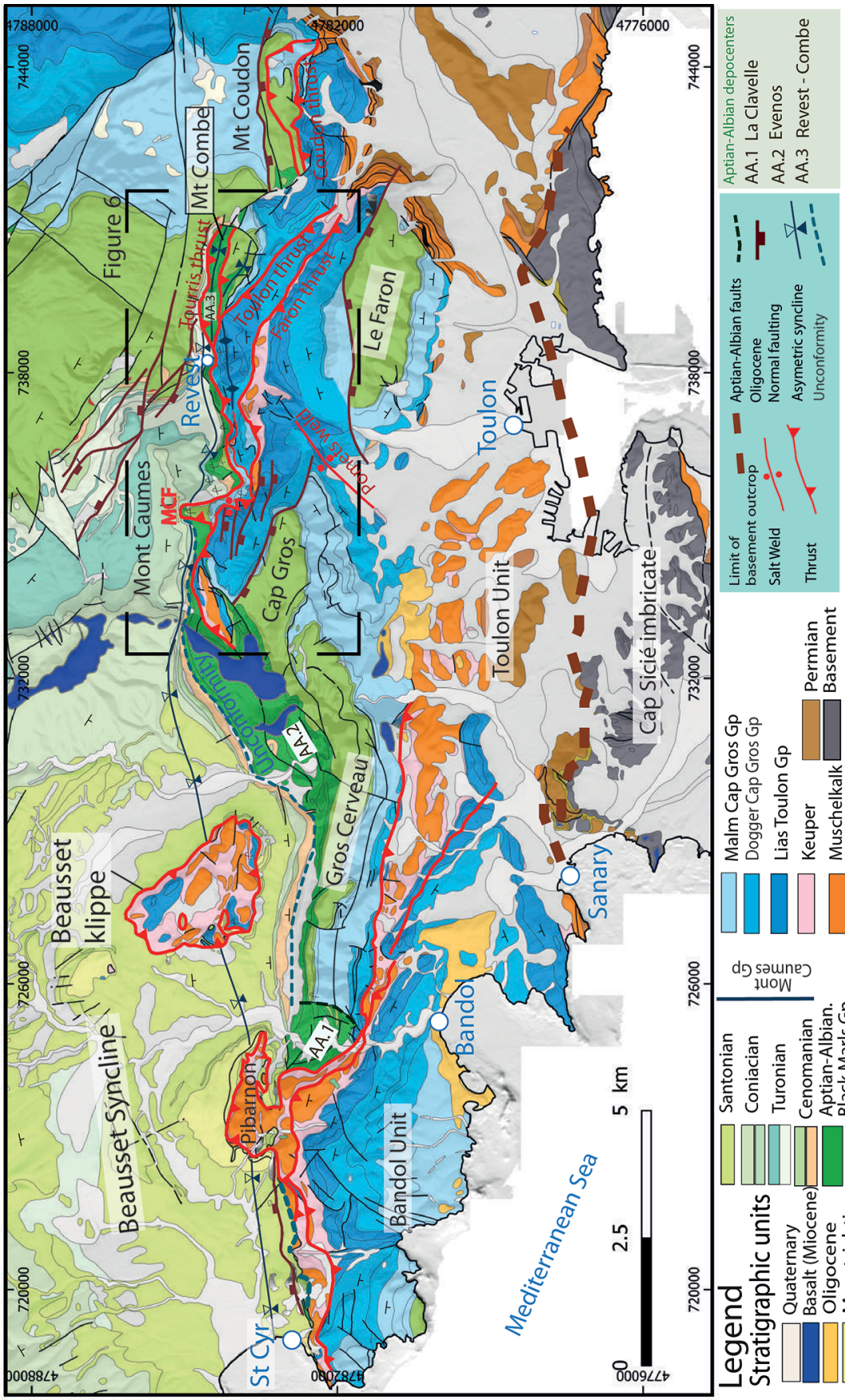

Fig. 2. Geological map of the Toulon Unit modified from the BRGM 1/50 000 Toulon map (Gouvernet *et al.*, 1969, 2nd ed.). The main study area is located north of Toulon between Mont Caumes and Le Revest in the Toulon Fault Zone (boxed area).

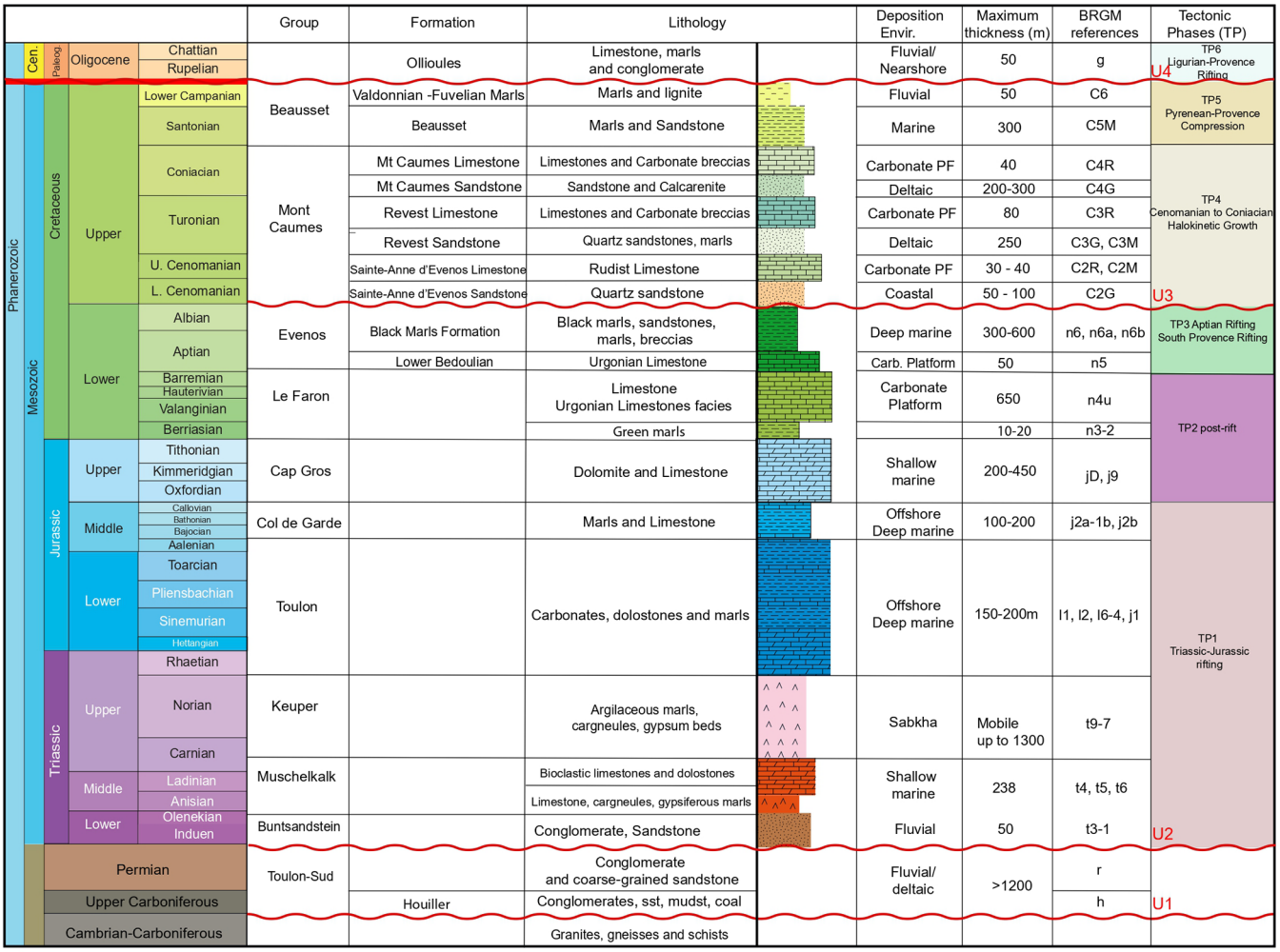

Fig. 3. Toulon Belt Lithostratigraphic table. Group names are proposed by the authors, formation names, maximum thicknesses at outcrop, principal unconformities (U1 to U4) and map codes are derived principally from BRGM maps and memoirs (Gouvernet *et al.*, 1969). Depositional environments are derived from literature and BRGM memoirs. The principal tectonic phases TP1 to TP6 are discussed in the text.

2 Geological setting

2.1 Southern Provence fold and thrust belt

The E-W trending Provence fold and thrust belt can be traced across southern France from the Pyrenean orogen to the southern Subalpine chains (Fig. 1). It has been extensively studied and mapped and has a well-established Mesozoic to Cenozoic stratigraphy (see Philip *et al.*, 1987, Bestani *et al.*, 2015, 2016; Espurt *et al.*, 2019 for summaries). In eastern Provence where the Mesozoic succession is some 3 km thick, asymmetric E-W synclines (Beausset, Arc and Rians) are delimited by major thrusts (Fig. 1; Espurt *et al.*, 2012; Bestani *et al.*, 2016). The Beausset Syncline (also known as the southern Provence Basin; Philip, 1970; Hennuy, 2003) is the most southerly of these synclines. It is overthrust from the south by the Coastal Inner Units, which preserve a Permian to Oligocene succession overlying Variscan basement that crops out in the Maures and Cap Sicié Massifs (Figs. 1 and 2; Espurt *et al.*, 2019). Estimates of Pyrenean-Provençal shortening across eastern Provence range from 25–30 km (Tempier 1987; Espurt *et al.*, 2019) to 46 km (Bestani *et al.*, 2016). Six major Triassic to present-day tectonic phases are well established in the literature and are used here to facilitate descriptions (TP1 to TP6; Fig. 3). The role of Triassic salt during each phase will be discussed.

Permian depocenters were formed during the transtensional break-up of Pangea and have a heterogeneous distribution across southern Provence mainly controlled by NNE to SE trending steeply dipping normal and strike-slip faults (Bathiard and Lambert, 1968; Delfaud *et al.*, 1989). From Middle Triassic to end Middle Jurassic, Tethyan rifting (Tectonic phase 1, TP1) affected all southern France and the western Mediterranean controlled principally by the NE-SW trending Cevenole fault system (Handy *et al.*, 2010; Tavani *et al.*, 2018). This was followed by post-breakup thermal subsidence of the margin through Late Jurassic and Early Cretaceous to Barremian (TP2). From Aptian to base Cenomanian, a second phase of oblique rifting was developed between Iberia and Europe from the Bay of Biscay to southern Provence (TP3; Philip *et al.*, 1987; Turco *et al.*, 2012; Sibuet *et al.*, 2004; Fournier *et al.*, 2016). A major E-W area of

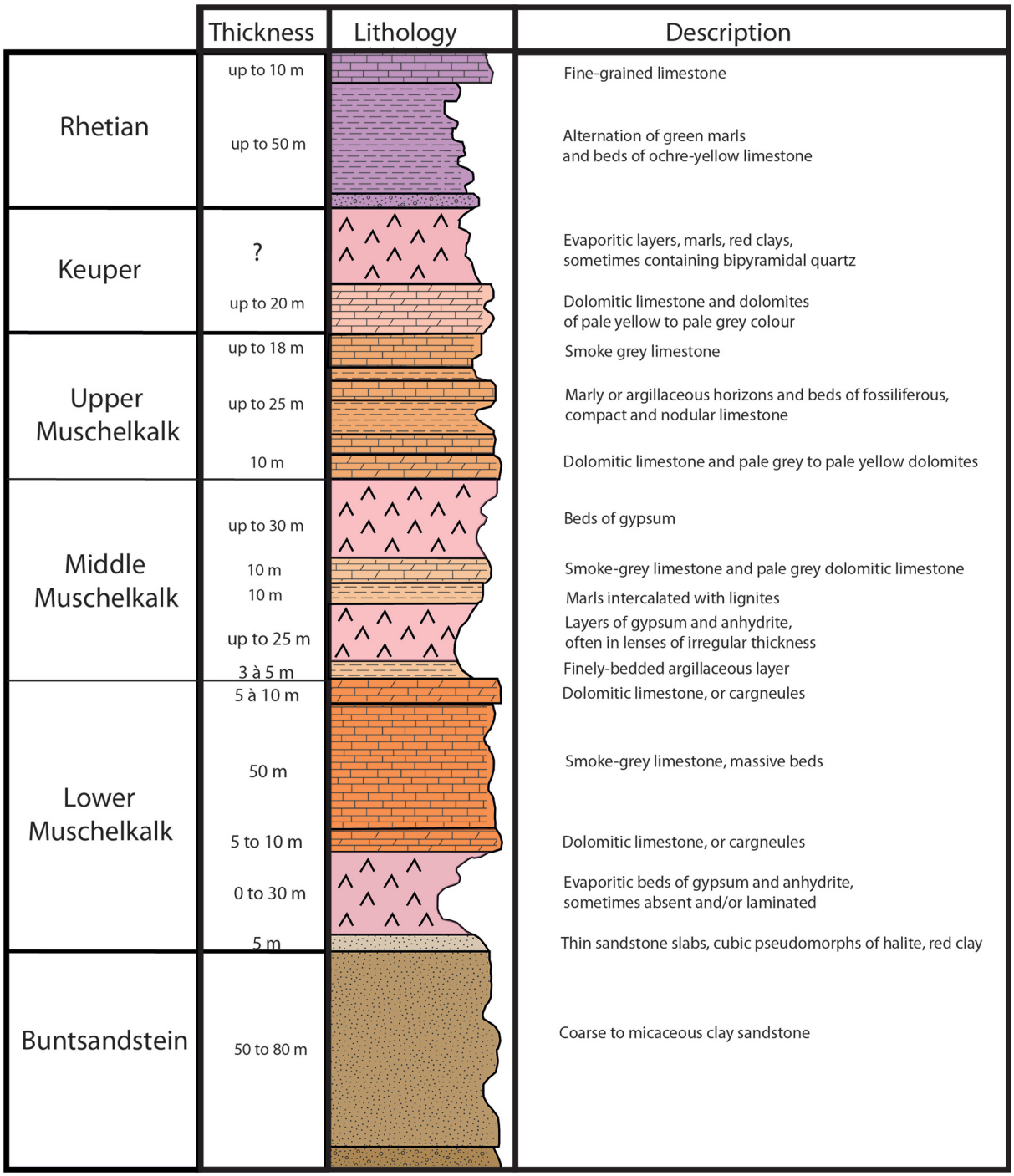

Fig. 4. Representative lithostratigraphic log of the Triassic of the Toulon area adapted from Caron and Laville (2016).

regional uplift, erosion and bauxite deposition, known as the Durancian high, was developed during Latest Albian and Early Cenomanian between the Pyrenean Rift System in Provence and the Vocontian Basin to the north (Masse and Philip, 1976; Chorowicz and Mekarnia, 1992; Guyonnet-Benaize *et al.*, 2010). During the early Late Cretaceous (Cenomanian, Turonian, Coniacian), the SE Beausset Basin was supplied with quartz-rich clastics from the south and east (Hennuy, 2003) derived from an uplifting basement massif known as the "Meridional Massif" believed to have been part of the paleo-Corsica-Sardinia block (TP4; Philip, 1970; Guieu *et al.*, 1987; Hennuy, 2003). The tectonic regime during this period is debated (Philip *et al.*, 1987; Hennuy, 2003) and will be investigated in detail in this contribution.

Plate reconstructions indicated that around 80–84 Ma, the African and Eurasian plates began to converge (*e.g.*, Handy *et al.*, 2010; Macchiavelli *et al.*, 2017). This led to the formation of the Pyrenean orogen between Iberia and Europe

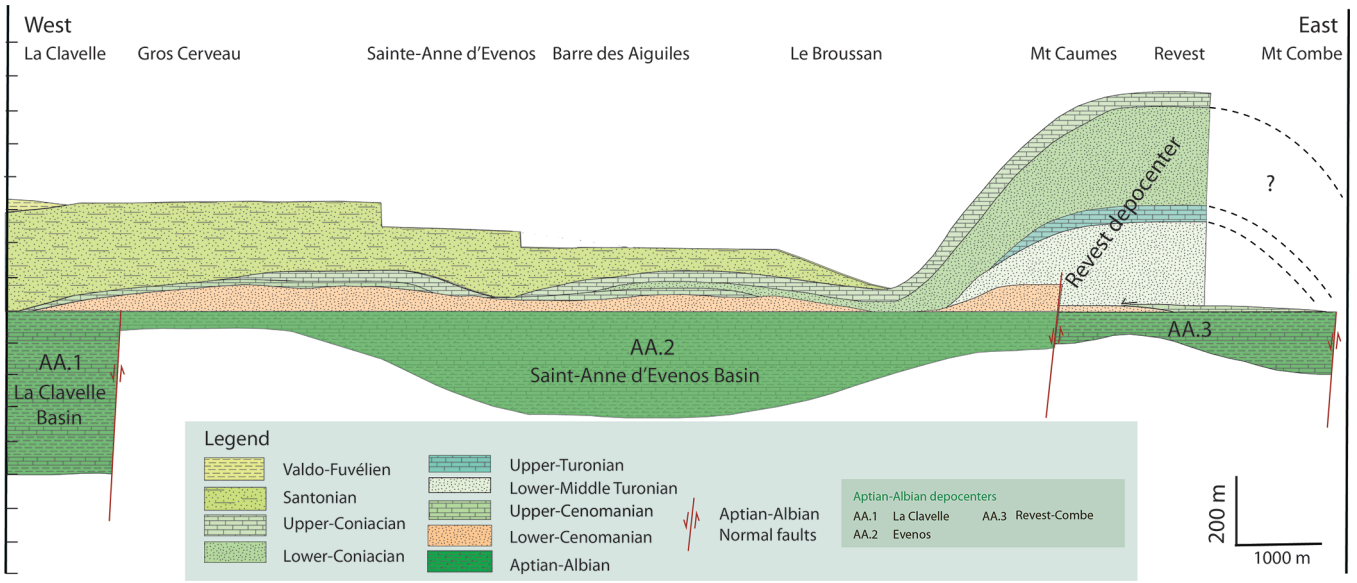

Fig. 5. E-W correlation of lithostratigraphic units of Aptian to Campanian age in the hinge zone and southern limb of the Beausset Syncline.

from latest Santonian to Miocene (Stampfli and Borel, 2002; Sibuet *et al.*, 2004). In Provence, Pyrenean deformation (TP5) migrated northward from at least Santonian to Eocene (40 Ma; Lacombe *et al.*, 1992; Le Pichon *et al.*, 2010; Espurt *et al.*, 2019 and references therein). To the south and east, subduction of oceanic lithosphere of the African plate beneath the European plate led to uplift of the Corsica-Sardinia block (Lacombe and Jolivet, 2005). However, the timing, geometry, position and kinematics of this subduction are strongly debated (see models of Vially and Trémolières, 1996; Roure and Choukroune, 1998; Lacombe and Mouthereau, 2002; Lacombe and Jolivet, 2005). The opening of the Liguro-Provençal Rift Basin from Oligocene to Burdigalian (TP6) destroyed much of the eastern portion of the Pyrenean orogen and strongly affected southern Provence (Hippolyte *et al.*, 1993; Mauffret and Gorini, 1996; Gattacceca *et al.*, 2007; Le Pichon *et al.*, 2010; Rangin *et al.*, 2010). The Maures-Esterel Basement Massif was uplifted on the Oligocene-Miocene rift shoulder (Jourdan *et al.*, 2018) (Fig. 1).

2.2 Coastal Inner Units

The Coastal Inner Units (Toulon and Bandol Units) are thrust northward over the Beausset Syncline along two evaporite and shale-rich fault zones, the Bandol Thrust and the Toulon Fault Zone linked by a NE-SW trending relay zone characterized by a base Cenomanian unconformity (Fig. 1c and 2). Marine Aptian-Albian and coastal Lower Cenomanian deposits are aligned along the whole northern margin of the Coastal Inner Units (Philip, 1970; AA1 to AA4, Fig. 2). The E-W trending Toulon Belt is 25 km long and 8 km wide (N-S). It comprises a series of faulted limestone massifs of Triassic to Lower Cretaceous strata up to 1000 m thick that show weak folding and tilting. Moving southward across the Toulon Unit, the erosion level cuts gradually downward into Permian strata and basement due to a regional tilting. The Mont Coudon, Le Faron and Cap Gros Massifs are defined by E to ENE trending south verging normal faults that preserve the youngest Urgonian limestones in their southern hanging-walls (Fig. 2). These are Oligocene-Miocene normal faults, which, along with local Miocene volcanism, are related to the opening of the Liguro-Provençal Rift Basin (Fig. 1c; Espurt *et al.*, 2019). The NE limb of the Beausset Syncline is cut by the N120 "Revest-Nord" Oligocene-Miocene normal fault dipping towards the north-east (RNF, Fig. 6). Oligocene-Miocene E-W to ESE-WNW extensional faults have been mapped offshore of the Maures Massif and Cap Sicié (Bellaiche *et al.*, 1971; Guieu and Roussel, 1990; Mauffret and Gorini, 1996).

The Bandol Belt consists of predominantly Jurassic strata lying in the open Bandol Syncline (Bestani *et al.*, 2016) and displaced northward on the Keuper-rich Bandol Thrust. The Pibarnon Half-Klippe and Beausset Klippe belong to the Bandol Thrust sheet (Fig. 2). They both comprise overturned Keuper, Muschelkalk and some Liassic strata that overlie Lower Campanian or Lower Santonian sediments of the Beausset Syncline (Bertrand, 1887; Haug, 1925; Gouvernet, 1963). To the south, the Cap Sicié Thrust sheet of Variscan basement and Permian red beds was emplaced northward during the Pyrenean-Provençal convergence (Bertrand, 1887; Haug, 1925; Espurt *et al.*, 2019). The periclinal E-W Beausset Syncline has a vertical to overturned southern limb and a north limb dipping on average 10°S. The unit is displaced northward by up to 7 km on the Sainte-Baume Thrust (Fig. 1c; Guieu, 1968; Bercovici 1983; Bestani *et al.*, 2015, 2016). The syncline preserves variations in thickness and facies in Aptian to Campanian strata (Philip *et al.*, 1987; Hennuy, 2003; Espurt *et al.*, 2019). Hennuy (2003) interpreted the Beausset depocenter as an oblique rift in which Albian to Santonian subsidence migrated eastward in the hangingwall of a north dipping, transtensional southern boundary fault while the

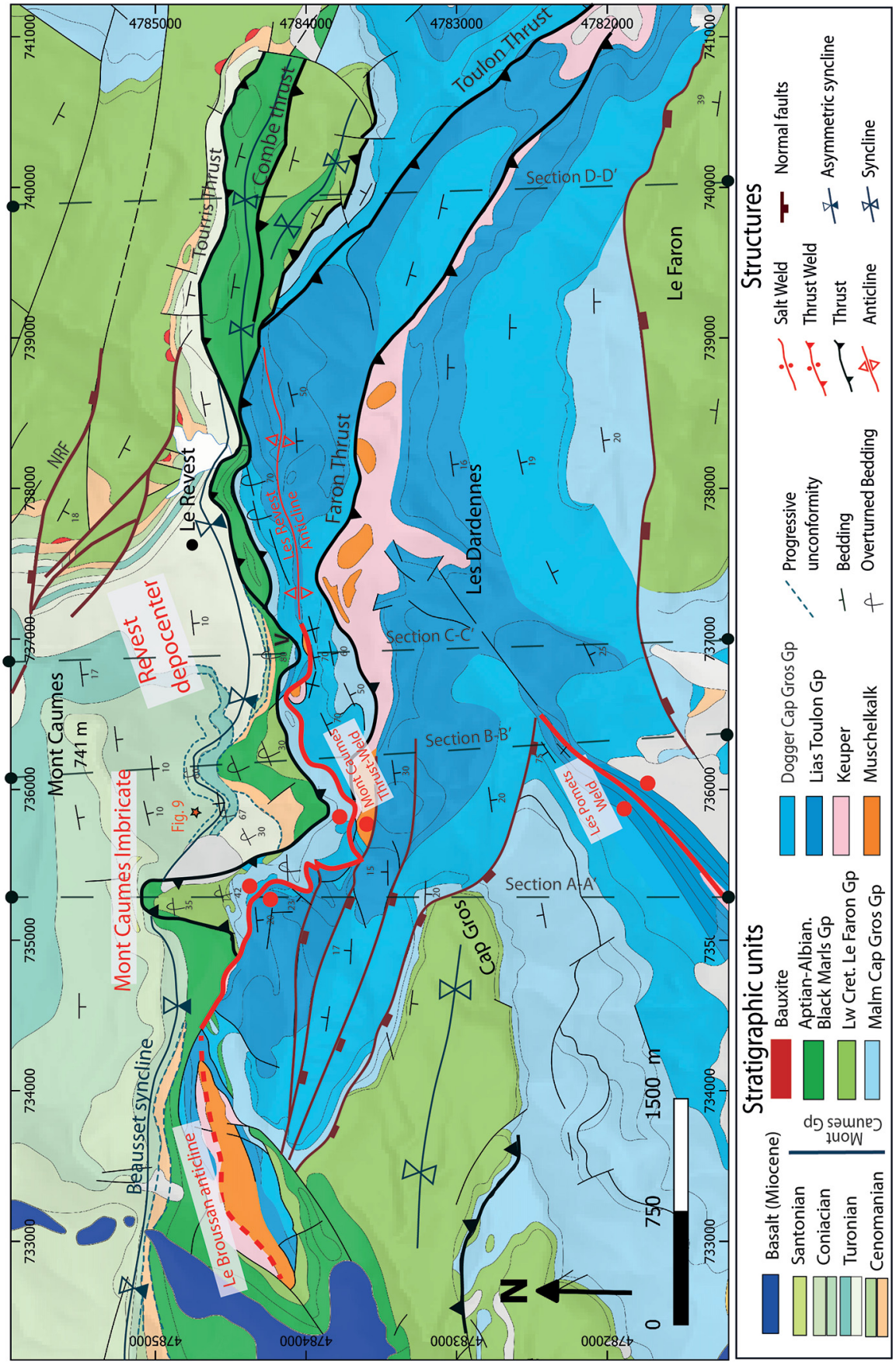

Fig. 6. Geological map of Mont Caumes – Revest area with our halokinetic interpretation and the main structures. The location of Sections A-A', B-B', C-C' (Fig. 7) and D-D' (Fig. 8a) are shown. Note the important thickness variation north of the Mont Caumes Weld and the overturned southern flank of the Beausset Syncline. Adapted from the 1/50 000 BRGM Toulon map (Gouvernet *et al.*, 1969).
Abbreviations: NRF: North Revest Fault; V: Mal Vallon; MCI: Mont Caumes Imbricate.

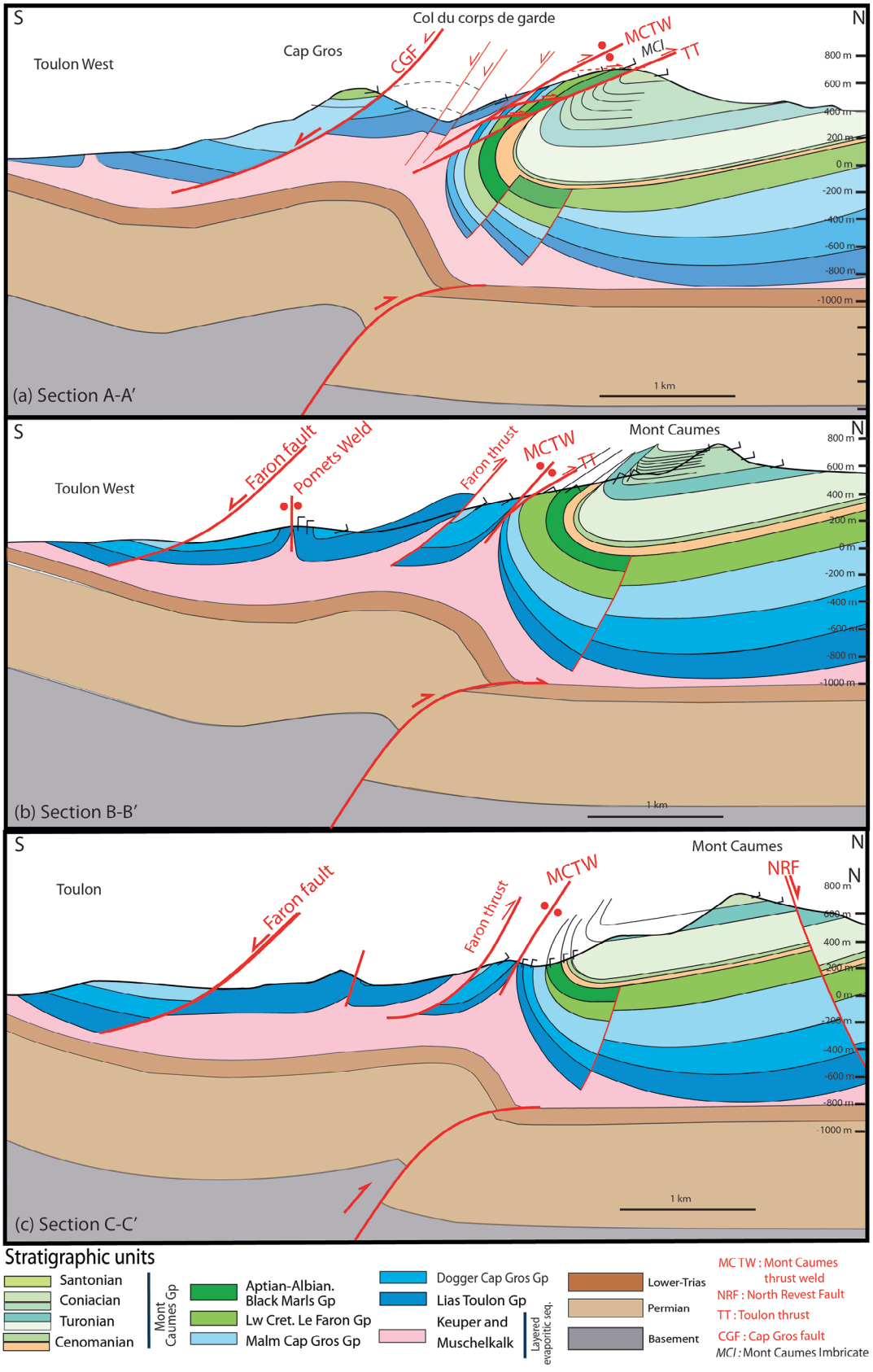

Fig. 7. Cross-sections and structural model proposed for eastern Toulon Fault Zone. (a) Section A-A'; (b) Section B-B'; (c) Section C-C'. For cross-section locations, refer to Figure 6 for location.

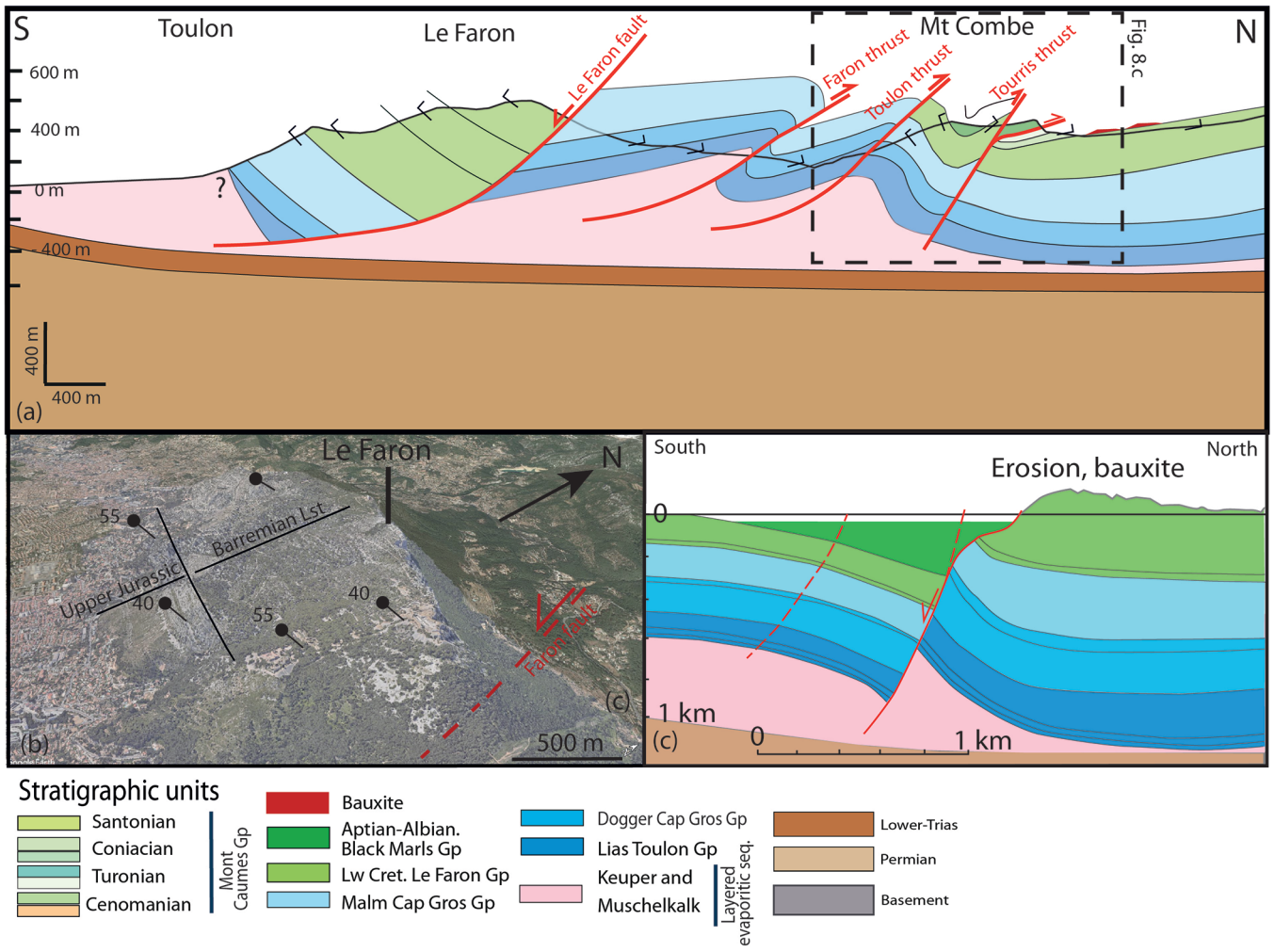

Fig. 8. (a) Cross-section D-D' for the eastern Toulon Belt located in Figure 6. (b) Google Earth image of the Le Faron Block showing steep northerly dips in Jurassic and Lower Cretaceous Units. (c) Schematic restoration of the Tourris block representing the Apto-Albian normal displacement.

"Meridional Massif" was uplifted in its footwall. In contrast, most other detailed tectono-stratigraphic studies propose that the Beausset Syncline was developed as an active synclinal depocentre during Late Cretaceous convergence (Philip, 1970; Philip *et al.*, 1987).

The structural framework and evolution of the Pyreneo-Provençal Belt and, in particular the Inner Coastal Units and Beausset area have been debated since the 19th century. The history of geological research in this area and its role in the evolution of conceptual models of orogenesis is presented in Philip (2012). Marcel Bertrand defined the concept of allochtonous nappes ("nappes de charriages") and large recumbent folds ("plis couchés") in Provence (Bertrand, 1887), identifying the Beausset Klippe as a remnant of an allochthonous recumbent north verging fold that is detached and thrust along Triassic evaporitic units. The Beausset Klippe was also thought to have an autochtonous origin (Toucas, 1873; Fournier, 1900). The allochtonous concept was also supported by the work of Haug (1925) in the Beausset area. In addition, Corroy and Denizot (1943) proposed for the first time that the Triassic Units were likely to pierce up to the surface and form recumbent anticlinal folds (Corroy and Denizot, 1943). Through these and other studies, southern Provence became identified as a type area for thin-skinned (or "cover") tectonics with Keuper and Muschelkalk evaporites acting as the principal décollement levels (*e.g.*, Philip *et al.*, 1987; Le Pichon *et al.*, 2010; Philip, 2012 and references therein). Other décollements levels were also identified within Middle Jurassic marls units and Aptian marls.

Recent studies have further elaborated on the role of Triassic evaporites in the deformation of eastern Provence (Bestani *et al.*, 2015; Caron and Laville, 2016; Espurt *et al.*, 2019). These authors propose three phases of diapirism. The first is characterized by passive diapirism from Jurassic to Cretaceous, the second is associated with the Pyrenean-Provençal convergence, and the third is due to Oligocene rifting. The proposed origin of early passive diapirism is variations in thickness of the Jurassic series due to Tethyan rifting. Diapir growth was therefore continuous from Early Jurassic to Santonian time, being particularly active during sinistral transtension during the Albian. The diapirs remained covered by Jurassic to Late Cretaceous strata, apart from the

Bandol diapir that pierced up to the surface during Middle to Late Cretaceous as evidenced at Saint-Cyr where the Santonian Unit is transgressive over Triassic Units (Philip, 1967) (Fig. 1). The emplacement of the Beausset Klippe over Campanian Units of the Beausset Syncline occurred during the Pyrenean-Provençal orogeny (Philip *et al.*, 1987; Philip, 2012). The third phase of is marked by reactivation of Mesozoic diapirs during Oligocene extension (Espurt *et al.*, 2019).

3 Stratigraphy

The sedimentary and stratigraphic framework of the Cretaceous Toulon and Bandol Units and Beausset Syncline is based on the detailed work of Philip (1967, 1970, 1980), Masse (1976), Machhour and Philip (1984), Mercadier (1984) and Philip *et al.* (1985, 1987) and the French Geological Survey (BRGM) maps and memoirs (Gouvernet *et al.*, 1969). The Permian to Oligocene formations are here arranged in lithostratigraphic groups that can be related to the six Triassic to present-day tectonic phases defined above (Fig. 3). The thicknesses given in this section and in Figure 3 represent maximum outcrop estimates, however thicknesses can be highly variable as will be documented below.

Variscan basement comprises Carboniferous granites, gneisses and schists (Maures and Cap Sicié Massifs). It is unconformably overlain by the Upper Carboniferous-Permian Toulon Sud Group consisting of a thin unit of Carboniferous deltaic clastic sediments (Houiller), followed by Permian red beds and volcanosclastics. On the western Maures Massif, the Toulon Sud Group reaches >1200 m (Bathiard and Lambert, 1968; Cassinis *et al.*, 2003). In the Toulon Unit, it is unconformably (U2, Fig. 3) capped by the 50 m thick Buntsandstein Group (Lower Triassic) consisting of medium to coarse fluvial sediments (Brocard and Philip, 1989; Durand and Gand, 2007).

The early phase of Tethyan rifting (TP1) is recorded by the Buntsandstein, Muschelkalk, Keuper, Toulon and Col de Garde Groups (Fig. 3). The Muschelkalk Group (Anisian-Carnian) is divided into three evaporite-carbonate systems schematically represented in Figure 4 (Caron, 1965a, 1965b, 1967a, 1967b, 1968; Caron and Laville, 2016; Espurt *et al.*, 2019). Limestones and dolomites of the Muschelkalk Group crop out principally in the Toulon Unit (Figs. 5 and 6) in discontinuous blocks surrounded by evaporites (mapped as Keuper). At outcrop, the Keuper Group (Carnian-Norian) consists of gypsum bed with beds of red clays, marls, dolomite and limestones, cargneules (de-dolomitised limestones) and rich in bipyramidal quartz crystals (Caron, 1968; Caron and Laville 2016). Keuper evaporites crop out principally along the Bandol Thrust, in the southern Toulon Unit and locally along the northern margin of the Toulon and Bandol Units. Traces of Keuper occur along many faults and welds. The thickness of this mobile and poorly exposed unit is difficult to constrain although estimations at outcrop are around 100 m (*e.g.*, Gouvernet *et al.*, 1969). In exploration, wells across eastern Provence, the Keuper, can however vary between 100 m and 200 m, reaching 1130 m in the Carcès-1 Well (Mennessier, 1959; Duvochel *et al.*, 1977; Baudemont, 1985; Espurt *et al.*, 2019).

From Late Triassic (Rhaetian) to end Middle Jurassic, the carbonates, dolostones and marls of the Toulon Group (max. 150 to 200 m, Rhaetian-Aalenian) and marls and marly limestones of the Col de Garde Group (max. 100–200 m, Bajocian-Callovian) were deposited on the deepening distal European margin during the opening of the Tethys oceanic domain (TP1). Continued post-break-up subsidence (TP2) is recorded by the Upper Jurassic Cap Gros Group and the Berriasian to Barremian Le Faron Group. The Cap Gros Group comprises shallow marine dolomites and limestones. These are 200–450 m thick at Le Faron, Cap Gros and Gros Cerveau Massifs (Figs. 6 and 7). They thin abruptly at the western end of the Gros Cerveau Massif in the La Clavelle block (Fig. 2). The Le Faron Group is made of a distinctive basal Green Marls Formation (marls and limestone, 10–15 m) overlain by a thick rudist-bearing carbonate platform (Valanginian to Barremian; Urgonian facies; Masse, 1976). The group is estimated at max. 650 m on Le Faron (top not preserved) but thins markedly westward to 120 m along the Gros Cerveau Massif where the upper limit is preserved and to the north. It is 200 m thick in the Tourris hangingwall and thickens across the fault to 300 m in the footwall (Fig. 8a).

Marine Aptian-Albian depocentres are aligned along the northern margin of the Coastal Inner Units (Philip, 1970; AA1 to AA3, Fig. 2). Apto-Albian outcrops are 1.5 to 4 km long and 1 to 1.5 km wide (N-S). N-S to SSW-NNE inverted and sealed Apto-Albian faults are observed in La Clavelle, Gros Cerveau, Évenos, Mont Caumes and east of Le Revest (Philip *et al.*, 1987). These depocentres have been described as graben separated by horsts (Masse and Philip, 1969; Philip *et al.*, 1987). Directly offshore to the west of the Bandol Unit and Cap Sicié Apto-Albian depocentres reaching 2000 m in thickness are also identified on seismic lines (Fournier *et al.*, 2016) associated with EW normal faults. These offshore basins appear to be overthrust by the Coastal Inner Units. The Apto-Albian Évenos Group consists of lowermost Bedoulian (earliest Aptian; n5 up to 50 m; Fig. 3) platform limestones with sparse rudists marking the gradual demise of the Urgonian platform overlain by marine black marls, shales and sandstones marking an abrupt deepening (n6; 300–600 m). The black marls can be subdivided into Middle Aptian dark grey marls with cherts and *orbitolina* and argillaceous limestones with ammonites (Lower Black Marls; n6a). Deepest conditions are evidenced in the uppermost Aptian (Clansayesian) to Upper Albian (Vraconian) Upper Black Marls (n6b), consisting of black marls with ammonites and planktonic foraminifera, glauconitic sandy limestones and glauconitic sandstones with chert (Tronchetti, 1981), which can reach 250 m in thickness. This unit can record gravitational instabilities with slumps, local unconformities and breccias of Urgonian limestones (Masse and Philip, 1969; Philip *et al.*, 1987; Machhour *et al.*, 1994). The total thickness of the Évenos Group is highly variable from east to west with a maximum of 650 m in the La Clavelle depocenter (AA1, Fig. 2) and 350 m in the Évenos depocenter (AA2, Fig. 2; Philip *et al.*, 1987). These two depocentres are interpreted as rift basins separated by a paleohigh with a condensed and/or eroded succession (Philip *et al.*, 1987 and references therein). Aptian carbonates are present along the north and NW rim of the Beausset Syncline (Hennuy, 2003). Both Aptian and Albian strata are however absent along the eastern and NE limbs where they are replaced

by an unconformity marked by bauxite deposits (Figs. 1c, 2 and 6).

An angular unconformity (U3) is recorded along the base of the Sainte-Anne-d'Évenos Sandstone Formation. The Cenomanian to end Coniacian Mont Caumes Group shows notable thickness and facies variations along the southern margin and eastern hinge zone of the Beausset Syncline (Fig. 6) (Philip, 1970; Hennuy, 2003). In contrast, on the northern limb of the Beausset Syncline the equivalent Cenomanian to end Coniacian stratigraphic succession comprises up to 200 m of carbonates (Philip, 1970; Hennuy, 2003).

In the Revest depocenter, the Mont Caumes Group, consisting of six formations of alternating (often lenticular) rudist carbonates and shallow marine to deltaic clastics, has a maximum cumulative thickness of some 700 m and records the fourth and most debated tectonic phase (TP4) (Figs. 3, 4 and 5; Masse and Philip 1976; Philip *et al.*, 1987; Floquet *et al.*, 2005, 2006). The quartz-rich clastic formations were supplied from the south, SE and east (Hennuy, 2003; Floquet *et al.*, 2006). The Early Cenomanian Sainte-Anne-d'Évenos Sandstone Formation (c2G) consists of quartzitic coastal sandstones (up to 50–100 m; Philip, 1970; Hennuy, 2003) which outcrop west and east of Mont Caumes. The Upper-Cenomanian Sainte-Anne-d'Évenos Limestone Formation is a discontinuous 30–40 m thick rudist limestone with some lignite intercalations marking the onset of a major marine transgression. The Lower-Middle Turonian Revest Sandstone Formation (c3G, c3M) is particularly thick in the Mont Caumes area, where up to 250 m of quartzitic cross-bedded calcarenites that were deposited in a prograding deltaic system (Philip, 1970; Hennuy, 2003). In the Mont Caumes area, the age of the base of the Revest Sandstone Formation remains unclear and sedimentation could have started during the Middle Turonian (Philip, 1970). This formation is overlain by the Middle to Upper Turonian Revest Limestone Formation made of rudist limestone and limestone breccias (80 m; Hennuy, 2003). The Turonian is thin or absent west of Mont Caumes (Fig. 5) (Hennuy, 2003). The Lower Coniacian Mont Caumes Sandstone Formation (quartz sandstone, conglomerate and calcarenite) is 200–300 m in the Mont Caumes area (Philip, 1970) and thins abruptly westward to pinch out at Sainte-Anne-d'Évenos (Fig. 5). The Upper Coniacian Mont Caumes Limestone Formation is made of up to 40 m of rudist limestone. It can be traced westward where it unconformably overlies Apto-Albian strata of the La Clavelle Basin (Fig. 2; Philip, 1970; Mercadier, 1984).

The Santonian Beausset Formation and the overlying Lower Campanian Valdonnian-Fuvelian Marls Formation were deposited during Pyrenean convergence (TP5) and are found only in the core of the Beausset Syncline to the west of our study area (Figs. 2 and 5). The Beausset Formation is up to 300 m thick and consists of shallow marine marls and marly sandstones with foraminifera and local layers of rudist limestones (Philip, 1970). Its base records a marine transgression across a surface that is locally unconformable notably to the west of the Pibarnon Half-Klippe (Fig. 2) where it overlies the Muschelkalk of the Bandol Unit (Fig. 2; Philip, 1967; Philip *et al.*, 1987; Espurt *et al.*, 2019). A transition from marine and continental conditions occurs at the base of the Lower Campanian Valdonnian-Fuvelian Marl Formation that is preserved only west of La Clavelle (Fig. 2). This formation consists of lacustrine argillaceous limestone with lignite beds and marls.

Liguro-Provençal rifting (TP6) is recorded in the Oligocene lacustrine and continental deposits of the Ollioules Formation and later Miocene volcanic units (flood basalts) that locally unconformably overlie the eroded Provençal fold belts (Fig. 2).

4 The Toulon Fault Zone

The 10 km long arcuate Toulon Fault Zone separates the eastern closure of the Beausset Syncline to the north from the Toulon Unit to the south (Figs. 2 and 3; Haug, 1925; Gouvernet, 1963). In this section, we describe and interpret the detailed structure and stratigraphy of the Toulon Fault Zone, Toulon Unit and southern Beausset Syncline (Figs. 1, 2 and 6). The text is illustrated by the detailed map in Figure 6, four cross-sections (Figs. 7 and 8), interpreted field photographs (Fig. 9) and a Google Earth image (Fig. 10). These cross-sectional models are based on published observations (*e.g.*, BRGM maps; Haug, 1925; Gouvernet, 1963; Bercovici, 1983) that have been validated in the field as well as new detailed field analyses. Our observations have led to a reinterpretation of the geological history of the area integrating a strong halokinetic influence. We here first present the principal structural features and their variation along strike. We then describe and interpret stratigraphic and structural data relevant for tectonic phases TP1-2, TP3 and finally TP4.

4.1 Present-day geometries

The Toulon Unit can be divided into the Tourris, Toulon and Faron fault blocks. The Faron and Toulon Thrusts die out to the E-SE as they curve from N90 to N140 (Fig. 6). Displacement transfers to the Brémone and Coudon Thrusts further east (Fig. 6; Espurt *et al.*, 2019). In the Faron Thrust sheet, a complete Jurassic (650–700 m) and Lower Cretaceous (Le Faron Group, >650 m) succession (Figs. 3, 6 and 8) overlies Keuper evaporites with numerous isolated Muschelkalk enclaves (Fig. 6). The thrust sheet is cut by the E-W Faron Fault dipping 30–35°S, a listric normal fault which downthrows the highly tilted hangingwall by up to 600 m (Fig. 8). The Faron Thrust branches westward onto the Mont Caumes Thrust weld (Fig. 6).

In the eastern Toulon Fault block, Jurassic strata form the E-W trending, north-facing Le Revest anticline with a steep to overturned north limb (Fig. 6). The fold tightens westward and is replaced by a tectonic contact that separates flanks with opposing vergence. We interpret this contact as a thrust weld because it has Keuper traces along its length, is associated with characteristic facies and thickness changes that will be described in detail below (Fig. 7) and, finally, it accommodates northward reverse displacement. The thrust weld is steep in the east (Fig. 7b) but shallows west as it curves through a marked right-stepping bend. At Col de Corps de Garde (Fig. 6), it dips 20°S and emplaces south dipping and younging Liassic Units above thin and overturned younger strata of the Mont Caumes flap (Fig. 7a). This flap in turn overlies the Toulon Thrust (Fig. 7a). West of the flap, the Toulon Thrust branches onto the thrust weld. Further west the N70 trending Le Broussan

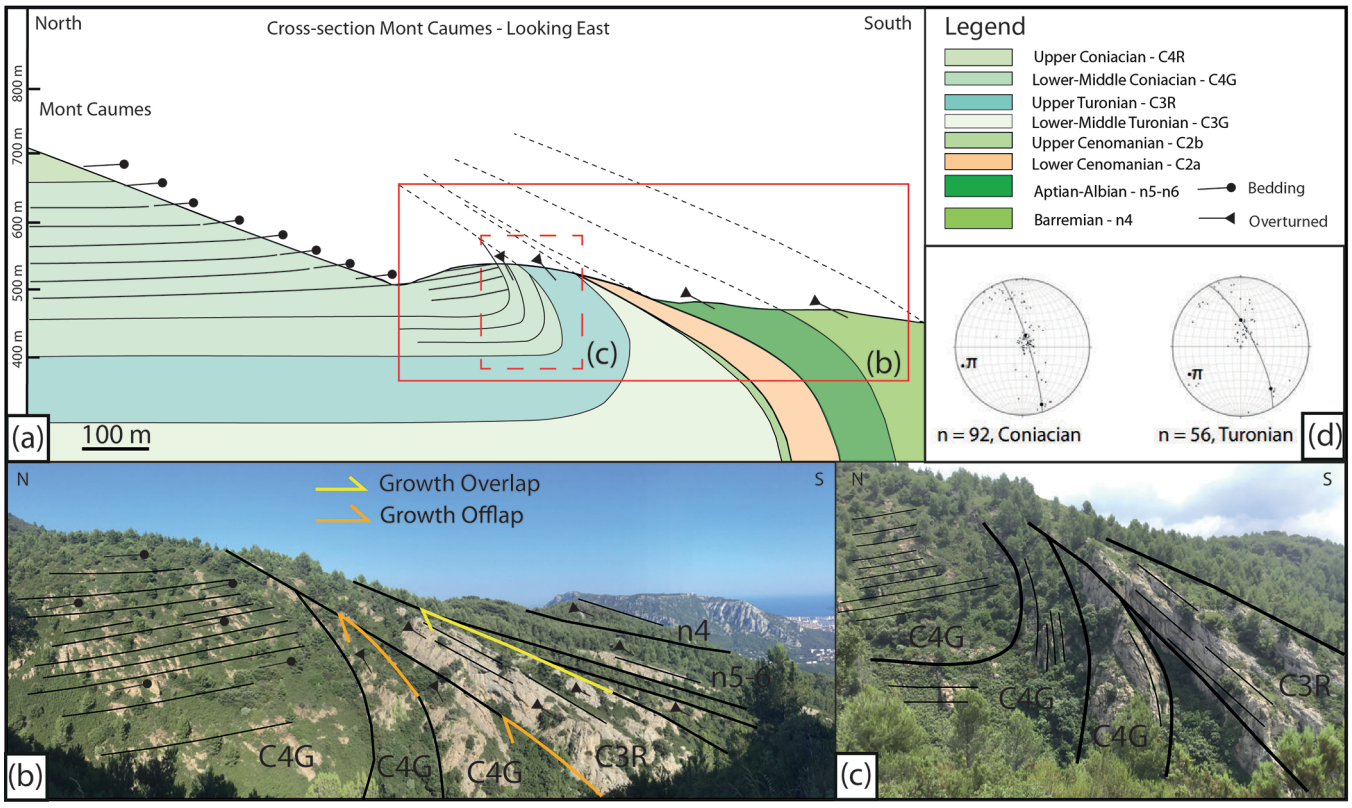

Fig. 9. Turonian-Coniacian stratal geometries of the Revest depocentre on the southern flank of Mont Caumes. (a) Growth strata and progressive unconformities in the hinge zone of the Beausset Syncline Revest depocentre. Part of Section B-B' looking east. (b) Field view looking east of the overturned southern limb and hinge zone of the Beausset Syncline and its associated progressive unconformities, wedges, and growth strata. (c) Stereonets of Coniacian and Turonian strata at Mont Caumes.

anticline lies in the immediately south of the thrust weld (Fig. 6; Haug, 1925; Gouvernet, 1963; Bercovici, 1983).

On the NE edge of the Toulon Belt, the steeply south dipping Tourris Thrust (Fig. 2; Espurt *et al.*, 2019) emplaces a popup of complexly folded and faulted Lower Cretaceous (Le Faron and Évenos Groups) strata (AA3 in Figs. 2, 5 and 8; Masse and Philip, 1973) against shallowly south dipping Lower Cretaceous beds (Le Faron Group) and Cenomanian Units (Fig. 8). The Middle Jurassic Cap Gros Unit below the popup is notably thin at 100 m in the Tourris Thrust hangingwall. Apto-Albian strata are absent in the footwall of the Tourris Thrust, replaced by an unconformity sealed by bauxite deposits. The Tourris Thrust links eastward with the Coudon Fault (Fig. 2), which is a gently reactivated steep normal fault that is still in net extension (Gouvernet, 1963). The Tourris Thrust branches westward onto the Toulon Thrust (Fig. 6). To the west of this branchline, Apto-Albian outcrops lie consistently in the footwall of the Toulon Thrust (Fig. 6).

The southern limb of the eastern Beausset Syncline consists of Aptian-Albian to Coniacian strata overturned to the north with complex internal unconformities and lateral and transverse thickness variations (Figs. 6, 7, 9 and 10) (Gouvernet, 1963; Bercovici, 1983; Philip *et al.*, 1987). At Mont Caumes, extremely overturned (15–20°S) and thin Jurassic to Aptian strata are displaced northward along the Toulon Thrust (Figs. 6, 7a and 10; Mont Caumes Thrust sheet of Bercovici, 1983; Gouvernet, 1963). The structure and stratigraphy in the footwall on the western and eastern sides of the Mont Caumes Thrust sheet are notably different (Figs. 6 and 10). The upper boundary of the Apto-Albian Évenos Group steps northward some 850 m to the west. In addition, the Turonian Units (Revest Sandstone Fm, Revest Limestone Fm) outcrop only to the east of the flap (Figs. 5 and 6). Finally, the axial trace of the Beausset Syncline steps northward going west below the flap (Fig. 6). Similarly, in the hangingwall of the Toulon Thrust, the Mont Caumes Thrust weld follows a right stepping curve immediately south the flap (Figs. 6 and 10). We deduce therefore that a NS to NNW-SSE trending feature must be associated with the flap at depth.

The southern flank of the Mont Caumes Thrust weld is cut by series of N90 to N110 trending normal faults located around the Col de Corps de Garde, dipping predominantly south (Figs. 6 and 7a). Fault traces are up to 3 km long (Fig. 6). These normal faults lie in the immediate footwall of the Cap Gros listric normal fault and together they accommodate downthrow to the south of some 500–550 m (Figs. 6 and 7a). The Cap Gros and Le Faron blocks are separated by an oblique NE-SW trending corridor where two oppositely younging series of steeply dipping Lower Jurassic Units lie back to back along a steep contact with traces of Keuper which we interpret as the Pomets salt weld (Figs. 2, 6 and 7b).

4.2 Triassic to Barremian stratal geometries (TP 1 and 2)

The combined Muschelkalk and Keuper Units represent a layered evaporite sequence (Rowan *et al.*, 2019) with an estimated thickness of 450 m comprising alternating strong (limestones, dolomites) and weak layers previously identified as multiple décollement horizons (Caron and Laville, 2016 and references therein). While gypsum is the main documented evaporite mineral at surface there is evidence that halite was also present (*e.g.*, pseudomorphs of halite, Caron and Laville, 2016) and it is reported in adjacent boreholes of eastern Provence (*e.g.*, Espurt *et al.*, 2019). However, it is impossible to determine exactly how much halite was originally in the succession. Isolated blocks of Muschelkalk carbonates are surrounded by poorly exposed evaporites indicating that the competent layers were variably ruptured and now lie within a mobile matrix consisting of connected evaporite layers (Figs. 4 and 6).

Jurassic and Lower Cretaceous Units are characterized by significant thickness variations, particularly around the Mont Caumes Thrust weld and the Pomets Weld (Figs. 7 and 8). On cross-sections A-A', B-B' and C-C', the Jurassic Units are projected down-plunge on the gently dipping northern limb of the Beausset Syncline from eastern outcrops assuming constant thickness (Fig. 3; 150–200 m, Toulon Group; 200 m, Col de Garde Group; 200–300 m, Cap Gros Group). However, immediately north of the Mont Caumes Thrust weld, the subvertical to overturned Toulon and Col de Garde Groups (Lias, Dogger) have a combined thickness of < 100 m (Figs. 3 and 6–8) while the Cap Gros Group (Malm) is 60 m thick in the overturned Mont Caumes Flap (Figs. 6, 7a and 10; Gouvernet, 1963; Bercovici, 1983). The Le Faron Group also thins and shows rapid along-strike variations, being completely absent at Mal Vallon (Fig. 6) shown on cross-section C-C' (Fig. 7c). We therefore represent a southward thinning of all Jurassic and Lower Cretaceous Units on the southern limb of the Beausset Syncline (Figs. 6 and 7), in other words toward the Mont Caumes Thrust weld. Immediately, south of the weld Jurassic thicknesses are deeply eroded and not well constrained. In the Cap Gros and Le Faron blocks, their thicknesses are similar to those on the northern limb of the Beausset Syncline (Figs. 7 and 8). On a larger scale, the Le Faron Group thins from east to west along the Gros Cerveau, thinning abruptly to < 100 m below the La Clavelle Apto-Albian depocenter (AA1, Fig. 2).

The NE-SW trending Pomets weld lies between the Cap Gros and Le Faron blocks (Figs. 2, 6 and 7a). The Toulon and Col de la Garde Groups thin toward the contact, which passes to the NE into a salt cored anticline described by Gouvernet (1963; Figs. 2 and 6). A thin Toulon Group succession becomes abruptly vertical to overturned on either side of this contact, forming back-to-back monoclines, typically observed along salt welds (Hudec and Jackson, 2007). The Hettangian Unit shows a distinct thickness difference between the two limbs (Figs. 7a and 7b; Gouvernet, 1963).

4.3 Aptian to Lower Cenomanian stratal geometries (TP3)

As summarized above, the Aptian-Albian Évenos Group records rifting along an EW zone that is preserved along the south limb of the Beausset Syncline (Philip *et al.*, 1987). To the east of Le Revest (Fig. 6), the group lies to the south of the Tourris Thrust (Masse and Philip, 1973) while to the north Aptian-Albian strata are absent, replaced by a bauxite-rich unconformity. We propose therefore that the Tourris Thrust represents an inverted normal fault that defined the northern margin of an Aptian-Albian rift depocenter (Figs. 6, 8a and 8c). West of Le Revest, the Évenos Group can be traced with variable thickness below the base Cenomanian unconformity (Philip, 1970) along the southern limb of the Beausset Syncline with a marked right step below the Mont Caumes Flap (Figs. 6 and 10). The northern margin of the rift must therefore lie uninverted at depth, implying that it was passively incorporated into the Beausset fold as shown on cross-sections in Figure 7. On section B-B' only, one normal fault defines the northern margin of the Aptian-Albian rift. A second normal fault on section A-A' can be observed at surface immediately east of the Mont Caumes flap (Fig. 6). This fault controls the Lower Cenomanian Sainte-Anne-d'Évenos Sandstone Formation that thins further east to 50 m on section B-B' and to only a few metres on section C-C' (Fig. 7).

4.4 Cenomanian to Coniacian stratal geometries (TP4)

The Cenomanian to Upper Coniacian Mont Caumes Group shows remarkable thickness and facies variations across the hinge and southern limb of the strongly asymmetric eastern Beausset Sycline (Figs. 5–7; Philip, 1970; Philip *et al.*, 1987; Floquet *et al.*, 2005; Floquet *et al.*, 2006; Hennuy, 2003). Quartz-rich shallow marine and deltaic clastics supplied from the east are overlain by and pass laterally into rudist-rich carbonate units to the north and west with breccia levels (Fig. 3; Hennuy, 2003). We refer to this area as the Revest depocenter in which the Mont Caumes Group has a maximum thickness of some 700 m and thins rapidly to the south and west (Figs. 5–7). Due to regional dips and erosion, the eastern limit cannot be constrained (Fig. 5). The NW-SE western edge of the depocenter has been described as an escarpment or paleorelief onto which Turonian and Coniacian Units onlap (*e.g.*, Philip, 1970; Hennuy, 2003), however it is largely hidden beneath the Mont Caumes Thrust sheet (Figs. 6 and 10). Further west, Turonian to Coniacian strata thin dramatically so that the Santonian lies directly on Lower Cenomanian west of Barre de la Jaume and on Muschelkalk at Pibernon (Figs. 2 and 5; Philip *et al.*, 1987; Philip, 2012; Espurt *et al.*, 2019). The southern synclinal limb comprises wedge-shaped packages of growth strata overturned to 20–30° S in oldest units (Figs. 6, 7, 9 and 10). Stratal wedges are separated by unconformities (Figs. 7 and 9). At the base of the group, the top of the Sainte-Anne-d'Évenos Sandstone Formation (C2G, Fig. 9) is onlapped by the Sainte-Anne-d'Évenos Limestone Formation (C2R) and a strongly upward tapering package of Revest Sandstone Formation (C3G) (Fig. 9). The top of the Revest Limestone Formation (C3R) is onlapped by strongly upward tapering packages of the Mont Caumes Sandstone Formation (C4G, Fig. 9). Finally, within the Mont Caumes Sandstone Formation (C4G), an angular unconformity separates an overturned package from gently dipping younger strata to the north that onlap the unconformity at near right angles within the synclinal hinge (Figs. 7b and 9). These varying stratal geometries and

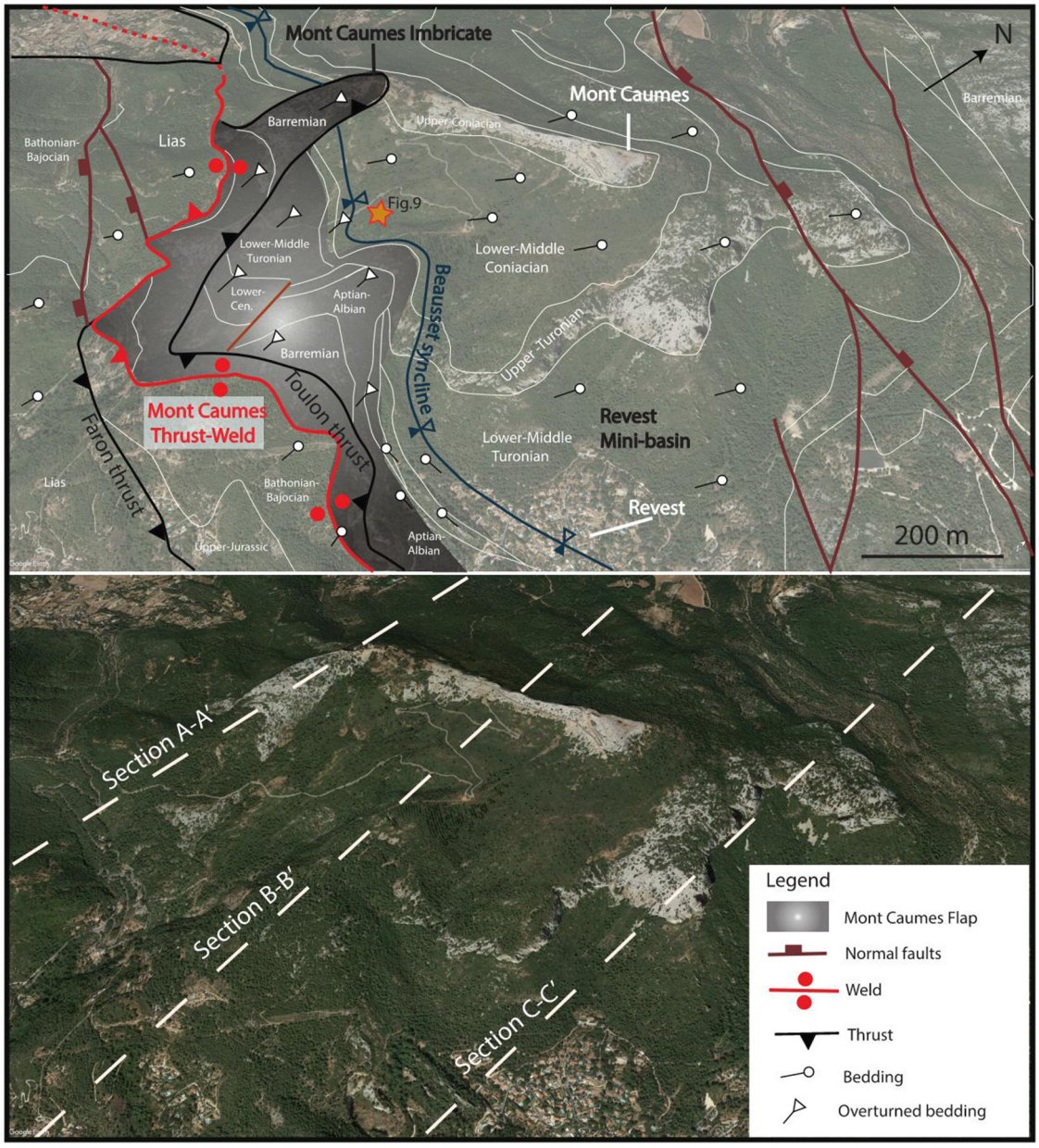

Fig. 10. Google Earth image of the Mont Caumes flap and Revest depocenter looking towards the north-west.

alternations between clastic and carbonate sedimentation document local variations in sedimentation rate, sediment supply and creation of accommodation during the Cenomanian, Turonian and Coniacian. The stratal geometries record active rotation of a fold limb which may be linked to either compressional folding or to rotation of the flank of a rising diapir. These possible origins will be discussed below.

On Mont Caumes, the southern flank of the Beausset Syncline is overlain by a remarkable overturned slice of thin Upper Jurassic to Aptian Units (Figs. 7a and 10) reported by Gouvernet (1963) and Bercovici (1983) as the Mont Caumes Thrust sheet (Figs. 6 and 10). This slice is 250 m to 600 m wide (E-W) and 1.4 km long (N-S) (Fig. 10). The Le Faron Group (Barremian) is only 60 m thick and the Cap Gros Group (Upper Jurassic) is less than 80 m thick while the combined Jurassic Units are no more than 100 m in total. The overturned slice lies between the Toulon Thrust and the Mont Caumes Thrust weld to the south (Fig. 7). These two low-angle thrusts are linked by low angle top-to-north shear zone (Fig. 7a) described by Bercovici (1983) and Gouvernet (1963).

5 Discussion

5.1 The role of salt in the evolution of the Inner Coastal Units

Across Alpine and Pyrenean domains a wealth of studies based on field and subsurface data document diapirism sourced mainly from the Keuper evaporites. These studies increasingly indicate that diapirism began in Jurassic times and continued

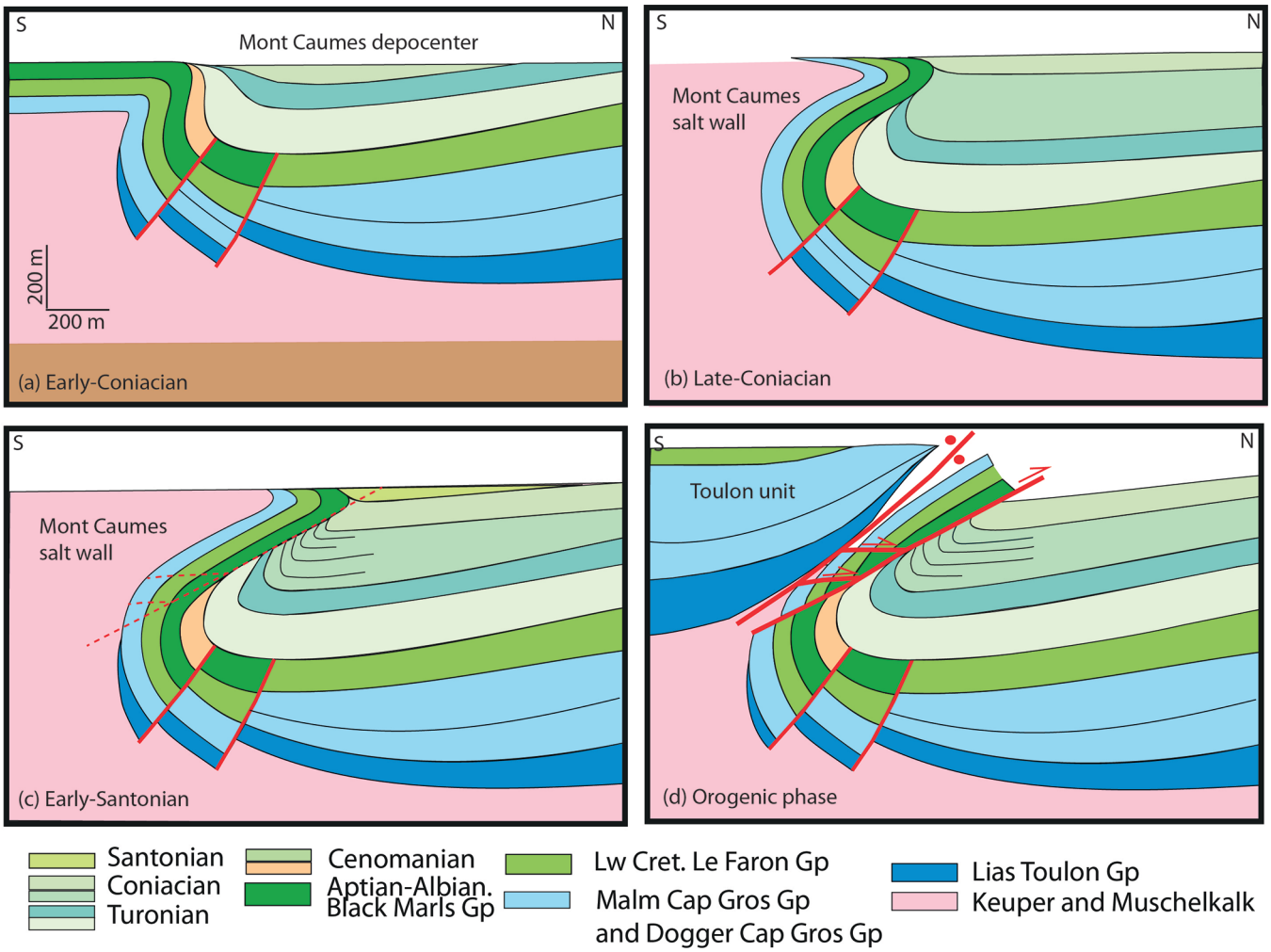

Fig. 11. Sequential restoration of cross-section A-A' (Fig. 7a) to (a) top Coniacian (c4G) and (b) top n4 (Barremian).

throughout the evolution of Tethyan and Pyrenean Rift Basins. Diapiric structures were commonly squeezed and inverted to form welds or salt-cored folds during alpine compression (*e.g.*, Canérot *et al.*, 2005; Graham *et al.*, 2012; Saura *et al.*, 2016; Cámara and Flinch, 2017; Célini *et al.*, 2020; Labaume and Teixell, 2020; Vergés *et al.*, 2020; Ford and Vergés, 2020). While diapirs are mainly sourced from Keuper evaporites, many authors also identify the mobility of underlying Muschelkalk evaporite layers. Notably, the early models of the Toulon Fault Zone identified the base of the Muschelkalk as the main décollement level (Gouvernet, 1963). The almost systematic fragmentation of competent Muschelkalk layers and their encasement in mobile evaporitic lithologies in the Toulon area (also commonly noted in other alpine fold belts), leads us to propose that the Keuper-Muschelkalk succession behaves as a mobile Layered Evaporite Sequence (LES; Davison *et al.*, 1996; Rowan *et al.*, 2016). The most commonly observed evaporite mineral in Keuper and Muschelkalk Units in Pyrenean and Alpine fold belts is gypsum (*e.g.*, papers in Soto *et al.*, 2017; Cámara and Flinch, 2017) as is the case in the Toulon Belt (Caron and Laville, 2016) where pseudomorphs of halite are also reported (Caron and Laville, 2016). Although gypsum is rheologically some ten times stronger than halite, it can still behave as a viscous, mobile material on geological time scales, its viscosity controlled by strain rate, temperature, presence of fluids (Davison *et al.*, 1996; Jackson and Hudec, 2017). While the composition and rheology of the Keuper-Muschelkalk LES in Provençal fold belts require detailed investigation, it is clear that this unit sourced diapiric structures during the Mesozoic.

Given the mobile nature of the Keuper-Muschelkalk LES Unit, we cannot constrain its original thickness. Caron and Laville (2016) suggest a value of 450 m (Fig. 4). However, they also recognize the presence of diapiric activity in the Toulon area. The highly variable present-day thicknesses of the Keuper-Muschelkalk LES represented on cross-sections (Figs. 7 and 8) are constrained by surface geology, and the principles of minimizing the volume of salt and the amount of shortening and earlier extension. Away from the Mont Caumes, diapir thicknesses vary from 200 to 450 m while diapir height is never more than 1 km. In Figures 11 and 12, we present the sequentially restored Toulon section A-A', using a halokinetic model, which will be argued at each step. Restoration assumes constant volume and bed length in suprasalt cover but no control can be applied to past volumes of the Keuper-Muschelkalk LES Unit. At every stage of

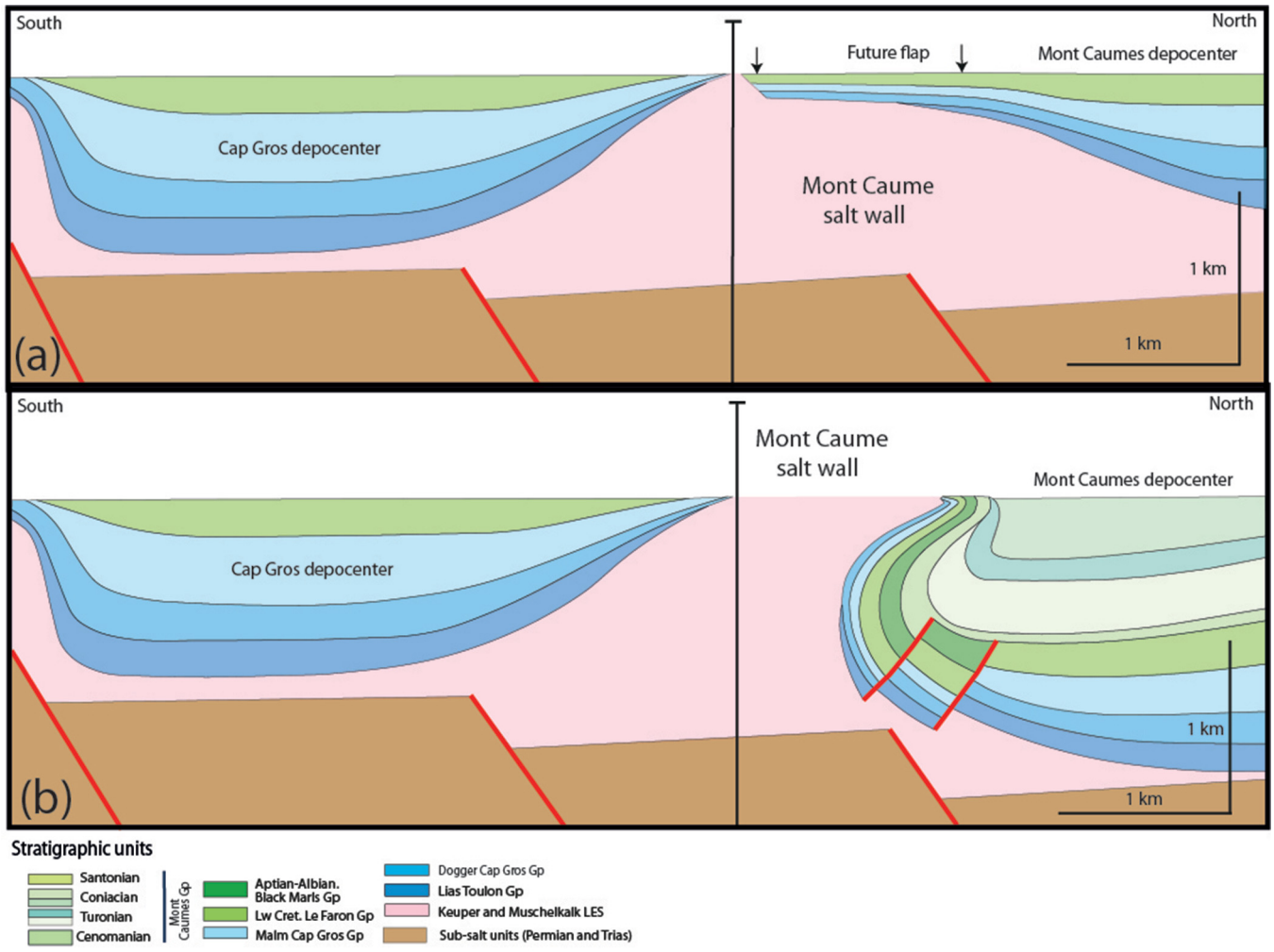

Fig. 12. Cartoon showing steps in the growth of the Mont Caumes Flap on cross-section A-A': (a) Early Coniacian; (b) Late Coniacian; (c) Early Santonian; (d) orogenic phase: Santonian.

Mesozoic evolution of the Inner Coastal Units, the Keuper-Muschelkalk LES decoupled deformation in the cover from that in the underlying basement. The degree of decoupling may vary in time and space.

Jurassic salt mobilization has been reported by Bestani *et al.* (2016) and Espurt *et al.* (2019) across eastern Provence, by Ford and Vergés (2020) in the eastern Pyrenees, by Vergés *et al.* (2020) in the Maestret Basin in the eastern Iberian Ranges, by Labaume and Teixell (2020) in the western Pyrenees and by Graham *et al.* (2012) and Célini *et al.* (2020) in the external French Alps. In the Toulon area, our data indicate that during the Jurassic and Early Cretaceous (TP1, TP2) a carbonate succession was deposited in broad synclinal depocenters controlled by gentle salt mobilization (Espurt *et al.*, 2019), stimulated by extension on underlying basement faults (Fig. 11). The Mont Caumes salt wall was located between the Toulon depocenter and the Revest depocenter to the north (Fig. 11a). We can only document with confidence the thinning of Jurassic to Lower-Cretaceous strata on the north side of the salt wall, where stratal geometries indicate that slow sedimentation rates (max. 0.005–0.007 mm/a) were greater than diapir growth rate.

From Aptian to Albian (TP3), the eastern Toulon Fault Zone represented the most easterly segment of the northern margin of an oblique rift system between Iberia and Europe (Philip *et al.*, 1987; Turco *et al.*, 2012). Distinct and relatively small Albian depocenters formed along this margin controlled by basinward (S) dipping normal faults (Figs. 11 and 12). The subsiding fault blocks expelled salt southward into the growing diapir (Worrall and Snelson, 1989; Jackson and Hudec, 2017). These depocentres were decoupled on evaporites from transtensional deformation in underlying basement.

The Mont Caumes Group represents a composite halokinetic succession deposited in the very restricted Revest depocenter where subsidence was controlled by growth of a 3D sinuous salt wall (Fig. 12). During the Turonian-Coniacian (92–87 Ma) subsidence locally accelerated to 0.14 mm/a over 5 Myrs to create this depocentre. Sequential restoration of the southern limb of the depocenter (Fig. 12) is constrained by thickness and dip data and stratal geometries (Figs. 7a and 9). The model shows halokinetic growth by drape folding on the northern margin of the passive Mont Caumes salt wall. The flap grew by progressive rotation of the limb combined with migration of the anticlinal hinge in a manner similar to that

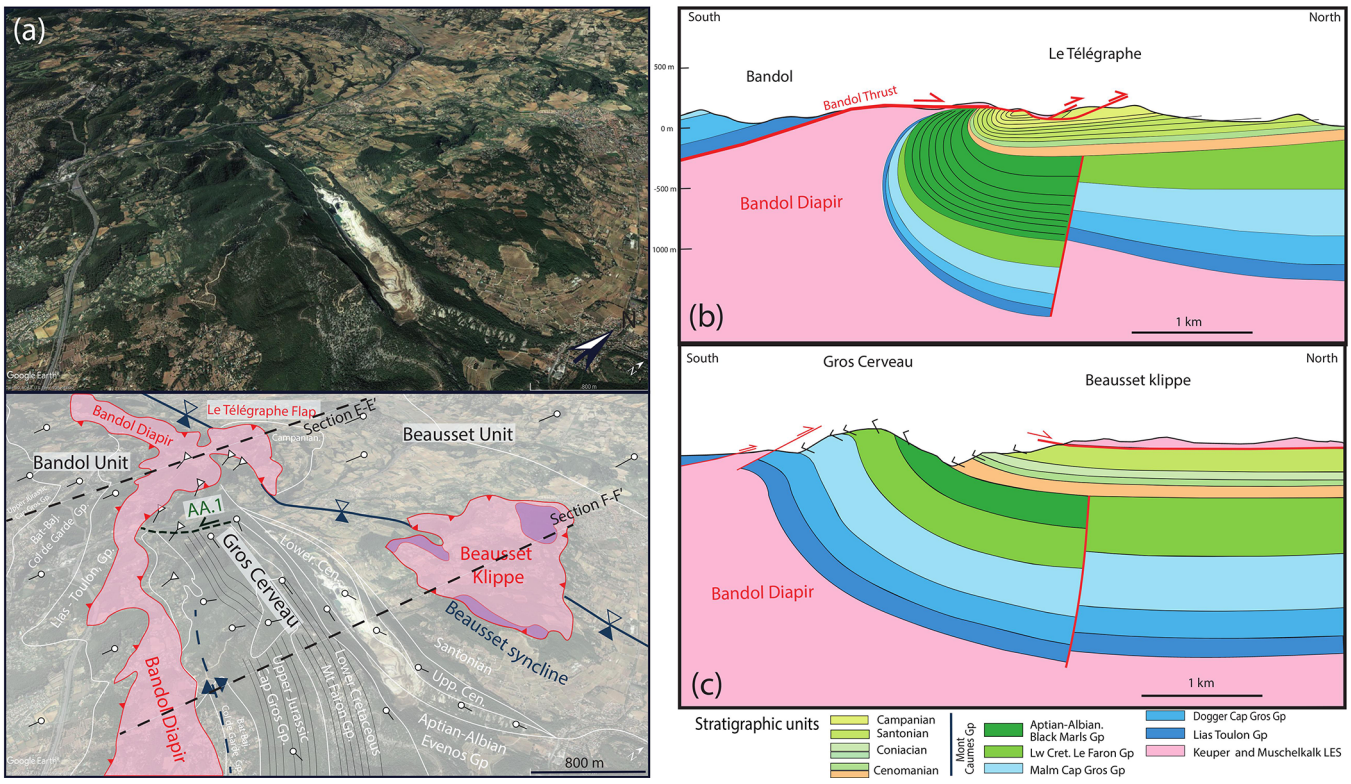

Fig. 13. The Bandol Unit and Bandol Thrust. (a) Google Earth view toward the west of the Bandol Thrust and western Beausset Syncline showing the Beausset Klippe and Pibernon Half-Klippe with uninterpreted view above and annotated view below. The location of cross-sections E-E' and F-F' are indicated. (b) Section E-E' showing the La Clavelle Apto-Albian depocentre, Bandol Thrust and Pibernon Half-Klippe. (c) F-F' cross-section showing the Bandol Thrust and Beausset Klippe.

observed in other well documented flap structures (Graham *et al.*, 2012; Rowan *et al.*, 2016). Flap growth accommodated the downbuilding of the depocenter as underlying salt was evacuated (Rowan *et al.*, 2016; Hudec and Jackson, 2007; Fig. 12). The intensity of flap growth increases from east to west as evidenced by progressively stronger overturning of Upper-Cenomanian to Coniacian beds and increasingly angular unconformities (Figs. 5, 6 and 10).

The amount of internal deformation in salt flaps is debated in the literature using field data, analog and numerical modelling (*e.g.*, Callot *et al.*, 2016; Rowan *et al.*, 2016). Rowan *et al.* (2016) notes that well documented natural examples record minimal bed lengthening (< 10%). In the Mont Caumes area, Bercovici (1983) and Philip *et al.* (1987) argue that the thin Jurassic and Cretaceous Units and the presence of horizontal shear zones were created by tectonic stretching of the steep to overturned limb of a Pyrenean-Provençal anticline with important horizontal shearing of the overturned limb as the anticlinal hinge zone was ruptured and the normal limb transported north on Triassic Units. This model cannot, however, explain the complex 3D stratal geometries reported here. It should also be noted that no horizontal shear zones are observed in the footwall of the Toulon Thrust (Fig. 9). While the presence and amount of layer-parallel stretching in the Mont Caumes flap remain to be more fully documented, we propose that the halokinetic flap developed on the northern flank of the Mont Caumes salt wall without significant internal deformation. The Mont Caumes imbricate was later sheared off the upper part of the flap (Fig. 12) and transported north between the Mont Caumes Thrust weld and the Toulon Thrust during Pyrenean-Provençal shortening with horizontal shear zones linking the two faults (Fig. 7a).

The Mont Caumes Group represents a composite halokinetic succession deposited in the very restricted Revest depocenter where subsidence was controlled by growth of a 3D sinuous salt wall (Figs. 6 and 12). As previously noted, the Mont Caumes imbricate is positioned at a significant right step in the trace of the Mont Caumes Thrust weld, in the Aptian-Albian depocentres and in the Beausset Syncline axial trace. It also coincides with the western termination of the Revest depocenter at depth (Hennuy, 2003). This conjuncture suggests long lived major three-dimensional feature curving from EW to NW-SE to EW, which we suggest may have been a sinuous salt wall now represented by the Mont Caumes Thrust weld. This geometry may have originally developed above a right stepping fault zone in basement.

5.2 The Bandol Thrust and associated structures

The north verging Bandol Thrust is the western equivalent of the Toulon Fault Zone (Figs. 1, 2 and 13). This thrust carries the salt-rich Bandol Unit, comprising > 1000 m of Jurassic strata, northward by an estimated 5 km (Espurt *et al.*, 2019).

Bestani *et al.* (2016) estimate some 20 km shortening on a cross-section passing through the Bandol Unit and the Bandol Thrust linking to a deeper basement thrust. In the footwall of the Bandol Thrust, the southern limb of the Beausset Syncline shows rapid lateral variations in stratal thicknesses, including the La Clavelle Apto-Albian depocenter underlain by very thin Jurassic Units (section E-E', Fig. 13), and further west again, the Saint-Cyr salt dome where Jurassic-Cretaceous strata are absent, and Santonian marine strata directly overlie Muschelkalk and Keuper Units (Philip *et al.*, 1987; Espurt *et al.*, 2019). In contrast to the Mont Caumes area, Turonian and Coniacian Units are very thin or absent at outcrop in the western Beausset Syncline (Figs. 5, 6 and 13; Philip, 2012 and references therein; Espurt *et al.*, 2019). Full section construction constrained by dip fans across the southern synclinal limb, demonstrates that no Turonian-Coniacian depocenter developed in the western Beausset Syncline (Fig. 13). The Bandol salt body, preserved in both the footwall and hangingwall of the Bandol Thrust appears to be considerably larger than that of Mont Caumes. It records a complex history including pre-Santonian emergence of the Saint Cyr dome (Philip *et al.*, 1987). Such early activity may have been contemporaneous with diapiric activity at Mont Caumes. The final emplacement of the Beausset Klippe and Pibarnon Half-Klippe (Figs. 1, 2 and 13) occurs during the Pyrenean-Provençal orogeny (Philip *et al.*, 1987). The mechanisms responsible for their emplacement are still debated, however, recent studies identify these allochthonous bodies as relics of an allochthonous salt sheet that flowed north from the extruding Bandol salt wall onto Santonian and Campanian strata of the Beausset Syncline (Bestani *et al.*, 2016; Espurt *et al.*, 2019).

5.3 Style and Timing of Pyrenean-Provençal deformation

Starting end Santonian, Pyrenean-Provençal N-S shortening of the Toulon cover was thin-skinned with faults rooting into the Keuper-Muschelkalk LES. Shortening (Figs. 11 and 12) increases from east to west reaching a maximum of some 2 km on section A-A' (Fig. 7a), mainly accommodated on the Mont Caumes Thrust weld and laterally equivalent structures. We identify the Mont Caumes Thrust weld as the principal tectonic boundary between the Toulon Unit and the Beausset Syncline. The Toulon Thrust is a second order structure in its immediate footwall which accommodated only 50–100 m displacement (Fig. 7). Our shortening estimate minimizes the width of the Mont Caumes salt wall (Fig. 11) and excludes the Cap Sicié basement thrust exposed to the south (Figs. 1 and 2), on which Espurt *et al.* (2019) estimate a displacement of some 14 km. In the same style as Bestani *et al.* (2016) and Espurt *et al.* (2019), we propose a basement thrust at depth below the Toulon Unit, which displaced top basement some 1.2 km to the north below Triassic evaporites (Figs. 7, 8 and 11). Emplacement of this basement unit passively raised the overlying cover units. It accommodates approximately the same shortening as the Mont Caumes Thrust weld (Fig. 11), however we cannot determine the exact relative timing of these suprasalt and subsalt structures. Cross-sections (Figs. 7 and 8) show displacement decreasing eastward on this basement fault from a maximum of 1.2 km on section A-A' (Fig. 7a), as it dies out eastward toward the western Maures Massif (Fig. 2). Additional northward tilting of top basement can be linked to uplift on the rift shoulder of the Oligocene Liguro-Provençal Rift Basin (Guieu and Roussel, 1990).

Below salt, we represent basement-involved structures, which accommodate alpine shortening on steep basement faults passing upward into forced folds in Permian cover as displacement on the fault dies out. Similar styles of basement involved structures are described in many foreland regions such as the Laramides, USA (McConnell, 1994; Mitra and Mount, 1998) and the Andes (*e.g.*, Allmendinger *et al.*, 2004) and have been simulated using trishear kinematic modelling (*e.g.*, Erslev, 1991; Hardy and Ford, 1997). Such south dipping basement faults may be inherited from Mesozoic rifting as suggested in Figure 1.

Although the history that we document here is in agreement with the timing and style proposed for southern Provence by Espurt *et al.* (2019), our detailed structural model differs in some key details. Most notably, on our cross-sections there is little difference between the maximum thickness of Jurassic successions of the Toulon Belt and those of the Beausset unit (500–700 m). In contrast, Espurt *et al.* (2019) propose a significant northward increase in Jurassic thicknesses from 500 m in the Toulon Unit to >1300 m in the Beausset Syncline, requiring the presence of a major north dipping basement-cutting normal fault between the two domains. No such major fault is required in our model and no major fault is documented in eastern outcrops along the basin margin. We propose instead that Jurassic-Cretaceous salt-controlled depocentres were decoupled from gentle thinning and subsidence of sub-salt basement (Fig. 12). As the Toulon and Beausset Units have been transported north several kilometres (Bestani *et al.*, 2016) cover structures no longer overlie original associated basement fault(s), which must lie somewhere to the south.

The relevance of the Turonian to Coniacian Revest depocentre for the timing of onset of Pyrenean convergence has long been debated (*e.g.*, Hennuy, 2003; Philip *et al.*, 1987; Espurt *et al.*, 2019). Based on the complex stratigraphic architectures, authors have speculated on a possible compression from the Late Albian to Early Cenomanian (Masse and Philip, 1976), or from Cenomanian to Turonian (Gouvernet, 1963; Bercovici, 1983; Philip *et al.*, 1987). If true, these structures would represent the earliest record of Pyrenean convergence in the most easterly outcrops of the orogen and be of major regional significance. This scenario would be consistent with growing evidence from field data and LT thermochronology that within the main body of the Pyrenean orogen deformation and uplift migrated from east to west (*e.g.*, Ternois *et al.*, 2019). However, recent studies have highlighted the role of Triassic evaporites in the deformation of the southern Provence (Bestani *et al.*, 2015; Espurt *et al.*, 2019) and therefore complex early structures may be adequately explained as halokinetic in origin without the need to invoke pre-end Santonian orogenic convergence. The new observations and analyses presented here provide significant new insight into the timing and drivers of this deformation.

Arguments for passive diapirism in the Mont Caumes area include the local and non-cylindrical nature of drape folding on the southern limb of the Revest depocenter, wedge-shaped,

unconformity-bounded stratal packages thinning upward that are identified as halokinetic sequences (Rowan *et al.*, 2016), the extremely rapid subsidence of the small Revest depocenter over a short period of time (5 Myrs). We conclude therefore that the Revest depocenter was created during the Late Cretaceous by salt evacuation and passive folding on the NE flank of the Mont Caumes salt wall. Its position in the core of the regional Beausset Syncline suggests that the Pyrenean-Provençal fold nucleated on this preexisting synclinal basin.

The onset of accelerated subsidence of the Revest depocenter correlates with the establishment of a new sediment source that supplied near-pure quartz sand into the Revest depocenter from Early Cenomanian to Late Coniacian (Hennuy, 2003). These sediments were derived from emerging basement massifs located somewhere to the E to SE, today represented by the Maures Massif, which, at the time, was attached to the Corsica-Sardinia block (Fig. 1; Turco *et al.*, 2012). Similarly, at La Ciotat on the NW limb of the Beausset Syncline (Fig. 1), deltaic sediments were supplied at this time from the south from the same new "Meridional Massif" (Hennuy, 2003), again believed to have been part the Corsica-Sardinia block. We suggest that the uplift and establishment of this new sediment source may be related to the onset of early subduction to the SE of the Corsica-Sardinia block (*e.g.*, Molli and Malavieille, 2011).

6 Conclusions

The Toulon-Bandol-Beausset area has been intensively studied since the first work of Marcel Bertrand in 1887. Numerous concepts and interpretation have been debated and developed in this complex area in particular the role of Triassic evaporitic units in the multiphase tectonic evolution of the region (Bertrand, 1887; Haug, 1925; Gouvernet, 1963; Philip *et al.*, 1987; Espurt *et al.*, 2019). The distribution, changing orientation and thickness of stratigraphic units, and multiple inter- and intra-formational progressive unconformities record an passively growing salt wall structure from Jurassic, with notable acceleration from Turonian to end Coniacian followed by Pyrenean-Provençal N-S shortening of Mesozoic cover on Triassic evaporites decoupled from deeper basement thrusting. The following conclusions summarize the halokinetic model and its regional significance.

1. The Toulon Fault Zone lies on the northern boundary of the Inner Coastal Units in the Pyrenean-Provençal fold belt. This area is within the Provençal Triassic evaporite domain where diapiric activity has been increasingly documented through the recognition of typical salt-related features such as flaps, welds and halokinetic depositional sequences as reported here. Diapirs were sourced from the pre-rift to early rift Triassic Muschelkalk-Keuper layered evaporitic sequence.
2. The Toulon Fault Zone is interpreted as having developed over tens of millions of years on the northern flank of the Mont Caumes salt wall that may have initially formed above a basement fault. Later northward translation has displaced cover structures with respect to original basement faults.
3. Slow carbonate sedimentation is recorded throughout the Jurassic and Early Cretaceous in broad synclinal depocenters controlled by gentle salt mobilization (Mont Caumes salt body).
4. A series of small marine rift depocentres have been developed during the Aptian and Albian along the northern flank of the Inner Coastal Units. These localized depocentres were controlled by normal faults of variable orientation dipping mainly basinward and toward known salt walls (Mont Caumes and Bandol). Depocentre subsidence evacuated salt toward the growing Mont Caumes salt wall. A sinistral transtensional regime on an underlying basement fault may explain the development of these basins.
5. During the Turonian and Coniacian accelerated asymmetrical growth of the Mont Caumes salt wall led to the development of the localized Revest depocenter supplied by a new sediment source area to the east and SE. The three-dimensional form and growth of the salt wall controlled rapid lateral stratal variations in the Revest depocenter including a westward increase in stratal overturning of a flap. Passive folding was accommodated by limb rotation and upward migration of the anticlinal hinge, thus lengthening the limb.
6. The Mont Caumes growth strata are therefore related to halokinetic passive folding rather than Early Pyrenean compressional folding.
7. Pyrenean-Provençal N-S compression initiated in the latest Santonian-earliest Campanian as elsewhere in the Pyrenees, squeezing and closing the Mont Caumes salt wall to form a thrust weld. The northern flank of the salt wall was thrust and sheared over the tightening Beausset Syncline.
8. Shortening of cover was decoupled along Triassic evaporites from basement thrusts at depth.
9. Oligo-Miocene normal faults linked to the opening of the Liguro-Provençal Rift Basin and rooting into Triassic evaporites cut the Inner Coastal Units, downthrowing blocks to the south.
10. The growth and inversion of the Mont Caumes salt wall and the larger Bandol salt wall further west controlled the evolution of the Inner Coastal Units.
11. While the history recorded here is coherent with more regional studies of Pyrenean-Provençal dynamics integrating halokinetic activity (*e.g.*, Espurt *et al.*, 2019), it reveals important details that allow us to distinguish halokinetic signals from deviatoric deformation and to better understand the interactions between regional and more local halokinetic strains.

Acknowledgements. This project was part of a MSc research project as part of the OROGEN project funded by Total, CNRS and the BRGM. We thank Laurène Bazinet for enthusiastic assistance during the field work, Nicolas Espurt, Hervé Sidèr, Antoine Crémadès, Naim Célini and Sébastien Ternois for many discussions and helpful comments. We are grateful to Jean-Paul Caron for discussion and for sending to us some useful historical documents. We also thank our colleagues of the OROGEN projects for their support and many stimulating discussions. We thank the two reviewers as well as the guest editors of the BSGF special publication, that considerably improved the content of this article.

References

Allmendinger RW, Zapata T, Manceda R, Dzelalija F. 2004. Trishear kinematic modeling of structures with examples from the Neuquén Basin, Argentina. In: McClay KR, ed. *Thrust tectonics and hydrocarbon systems*. AAPG Memoir 82, pp. 356–371.

Bathiard M, Lambert C. 1968. Rapports entre la tectonique de socle et la tectonique de couverture sur la bordure ouest des Maures. *Bull. Soc. Geol. Fr.* 7: 428–435.

Baudemont D. 1985. Relations socle-couverture en Provence orientale. Évolution tectonosédimentaire permienne du bassin du Luc (Var). Thèse de l'Université Louis Pasteur, Strasbourg, 204 p.

Bellaiche G, Mascle J, Recq M. 1971. Interpretation géologique des profils sismiques réalisé au sud du massif Maures. *Comptes rendus de l'Académie des Sciences, Paris, Série D*, 272.

Bercovici C. 1983. Contribution à la géologie de la région nord-toulonnaise. Structure de la région du Broussan-Dardennes. Cartographie détaillée et interprétation. Thèse de 3^{e} cycle, Université de Provence, 86 p.

Bertrand M. 1887. Ilot triasique du Beausset (Var). Analogie avec le bassin houiller franco-belge et avec les Alpes de Glaris. *Bulletin de la Société géologique de France* 3(XV): 667–702.

Bestani L, Espurt N, Lamarche J, Floquet M, Philip J, Bellier O, *et al.* 2015. Structural style and evolution of the Pyrenean-Provence Thrust Belt, SE France. *Bulletin de la Société géologique de France* 186(4-5): 223–241. https://doi.org/10.2113/gssgfbull.186.4-5.223.

Bestani L, Espurt N, Lamarche J, Bellier O, Hollender F. 2016. Reconstruction of the Provence Chain evolution, southeastern France. *Tectonics* 35(6): 1506–1525. https://doi.org/10.1002/2016TC004115.

Brocard C, Philip J. 1989. Précisions stratigraphiques sur le Trias de la Provence orientale : conséquences structurales et paléogéographiques. *Géologie de la France* 3: 27–32.

Callot JP, Salel JF, Letouzey J, Daniel JM, Ringenbach JC. 2016. Three-dimensional evolution of salt-controlled minibasins: Interactions, folding, and megaflap development. *AAPG Bulletin* 100 (9): 1419–1442. https://doi.org/10.1306/03101614087.

Cámara P, Flinch JF. 2017. The southern Pyrenees: A salt-based fold-and-thrust belt. In: Soto JI, Flinch JI, Tari G, eds. *Permo-Triassic Salt Provinces of Europe, North Africa and the Atlantic Margins*, pp. 395–415. https://doi.org/10.1016/B978-0-12-809417-4.00019-7.

Canérot J, Hudec MR, Rockenbauch K. 2005. Mesozoic diapirism in the Pyrenean orogen: Salt tectonics on a transform plate boundary. *AAPG Bulletin* 89(2): 211–229. https://doi.org/10.1306/09170404007.

Caron J-P. 1965a. Sur la position tectonique du Trias moyen de la région toulonnaise. *Comptes-Rendus l'Académie des Sciences de Paris* 260: 5069–5072.

Caron J-P. 1965b. Le Muschelkalk du mont Faron, près Toulon (Var). *Annales de la Faculté des Sciences, Marseille* XXXVII: 39–55.

Caron JPH. 1967a. Étude pétrographique, stratigraphique et paléo-océanographique du Muschelkalk supérieur calcaire de la région toulonnaise. Thèse Université de Marseille, 2 vol, 217 p., inédit.

Caron JPH. 1967b. Étude stratigraphique du Muschelkalk supérieur calcaire et dolomitique de Basse-Provence occidentale entre Bandol et Hyères (Var). *Bulletin de la Société géologique de France* 9: 670–677.

Caron JPH. 1968. Mise en évidence du Muschelkalk inférieur dans la région toulonnaise (Var). *Comptes-Rendus l'Académie des Sciences de Paris* 266(D): 1699–1701.

Caron JPH, Laville P. 2016. Paradoxes and inaccuracies in the geological maps of scale 1/50 000, which show the Upper Cretaceous of the southern margin of the basin of Le Beausset (Provence, France). *Boletin Geologico y Minero* 127(2-3): 517–526.

Cassinis G, Durand M, Ronchi A. 2003. Permian-Triassic continental sequences of Northwest Sardinia and South Provence: Stratigraphic correlations and palaeogeographical implications. *Bollettino Della Societa Geologica Italiana* 2(1): 119–129.

Célini N, Callot JP, Ringenbach JC, Graham R. 2020. Jurassic salt tectonics in the SW Sub-Alpine fold-and-thrust belt. *Tectonics* 39 (10): 0–3. https://doi.org/10.1029/2020TC006107.

Chorowicz J, Mekarnia A. 1992. Mise en évidence d'une extension albo-aptienne orientée NW-SE en Provence (Sud-Est de la France). *C.R. Acad. Sci. Paris, Série II* 315: 861–866.

Choukroune P, Mattauer M. 1978. Tectonique des plaques et Pyrénées ; surle fonctionnement de la faille transformante nord-pyrénéenne ; comparaisons avec des modeles actuels. *Bulletin de la Société géologique de France* 7: 689–700. https://doi.org/10.2113/gssgfbull.S7-XX.5.689.

Corroy G, Denizot G. 1943. La Provence occidentale. Géologie régionale de la France. Paris : Hermann et Cie, 182 p.

Dardeau G, de Granciansky P-C. 1990. Halocinèse et rifting téthysien dans les Alpes-Maritimes (France). *Bull. Cent. Rech. Explor. Prod. Elf Aquitaine* 14: 443–464.

Davison I, Alsop GI, Blundell DJ, eds. 1996. Salt tectonics. *Geological Society Special Publication* 100: 310.

Delfaud J, Toutin-Morin N, Morin R. 1989. Un cône alluvial en bordure d'un bassin intramontagneux : la formation permienne du Rocher de Roquebrune (Bassin du Bas-Argens, Provence orientale). *C. R. Acad. Sci, Ser. II: Mec, Phys, Chim, Sci. Terre Univers* 309: 1811–1817.

Durand M, Gand G. 2007. Le Permien et le Trias du Dôme de Barrot (Alpes-Maritimes). In: *Livret-guide de l'excursion annuelle de l'Association des Géologues du Permien et du Trias, 18-20 septembre 2007*, 26 p. https://www.researchgate.net/publication/321293102.

Duvochel P, Ferrandini J, Laville P. 1977. Lithologie et interprétation du sondage de Garéoult (Var) dans son cadre structural. *Bulletin du B.R.G.M, 2^{e} Série, Sect. 1* 4: 333–340.

Erslev EA. 1991. Trishear fault-propagation folding. *Geology* 19: 617–620.

Espurt N, Hippolyte J-C, Saillard M, Bellier O. 2012. Geometry and kinematic evolution of a long-living foreland structure inferred from field data and cross-section balancing, the Sainte-Victoire System, Provence, France. *Tectonics* 31(4). https://doi.org/10.1029/2011TC002988.

Espurt N, Wattellier F, Philip J, Hippolyte JC, Bellier O, Bestani L. 2019. Mesozoic halokinesis and basement inheritance in the eastern Provence fold-thrust belt, SE France. *Tectonophysics* 766(December 2018): 60–80. https://doi.org/10.1016/j.tecto.2019.04.027.

Fiduk JC, Rowan MG. 2012. Analysis of folding and deformation within layered evaporites in Blocks BM-S-8 and -9, Santos Basin, Brazil. *Geological Society, London, Special Publications* 363(1): 471–487. https://doi.org/10.1144/SP363.22.

Floquet M, Gari J, Hennuy J, Léonide P, Philip J. 2005. Sédimentations gravitaires carbonatées et silicoclastiques dans un bassin en transtension, séries d'âge cénomanien à coniacien moyen du Bassin sud-provençal. In: *Livret-guide d'excursion géologique, 10^{e} congrès français de sédimentologie, 14–15 octobre 2005*, Publication ASF, Paris, vol. 52, 80 p.

Floquet M, Philip J, Léonide P, Gari J. 2006. Sédimentation et géodynamique du bassin Sud-Provençal au Crétacé supérieur ; Histoire et dynamique des plates-formes carbonatées et de leur biotas durant le Phanérozoïque. In: *Livret-guide d'excursion*

géologique, Université de Provence, Marseille, 69 p. Livre en dépôt à la Soc. géol. France.

Ford M, Vergés J. 2020. Evolution of a salt-rich transtensional rifted margin, eastern North Pyrenees, France. *Journal of the Geological Society* 3: jgs2019-157. https://doi.org/10.1144/jgs2019-157.

Fournier E. 1900. Étude synthétique sur les zones plissées de la Basse-Provence. *Bulletin de la Société géologique de France* 28(3): 927–985.

Fournier F, Tassy A, Thinon I, Munch P, Cornée JJ, Borgomano J, *et al.* 2016. Pre-Pliocene tectonostratigraphic framework of the Provence continental shelf (eastern Gulf of Lion, SE France). *Bulletin de la Société géologique de France* 187(4-5): 187–215. https://doi.org/10.2113/gssgfbull.187.4-5.187.

Gattacceca J, Deino A, Rizzo R, Jones DS, Henry B, Beaudoin B, *et al.* 2007. Miocene rotation of Sardinia: New paleomagnetic and geochronological constraints and geodynamic implications. *Earth and Planetary Science Letters* 258(3-4): 359–377. https://doi.org/10.1016/j.epsl.2007.02.003.

Gouvernet C. 1963. Structure de la région toulonnaise. Mémoire de la Carte Géologique détaillée de la France, 244 p.

Gouvernet C, Blanc JJ, Philip J, Caron JP, Coulon C, Gueirard S, *et al.* 1969. Carte et notice géologiques Toulon à 1/ 50 000, 2^{e} éd. Service de la Carte géologique de la France.

Graham R, Jackson M, Pilcher R, Kilsdonk B. 2012.Allochthonous salt in the sub-Alpine fold-thrust belt of Haute Provence, France. *Geological Society, London, Special Publications* 363(1): 595–615. https://doi.org/10.1144/SP363.30.

Guieu G. 1968. Étude tectonique de la région de Marseille. Thèse de doctorat d'État, Marseille, 604 p.

Guieu G, Roussel J. 1990. Arguments for the pre-rift uplift and rift propagation in the Ligurian-Provençal Basin (Northwestern Mediterranean) in the light of pyrenean provençal orogeny. *Tectonics* 9(5): 1113–1142.

Guieu G, Philip J, Durand J-P, Nury D, Redondo C. 1987. Le détritisme provençal du Crétacé moyen à l'Oligocène dans son cadre paléogéographique, structural et géodynamique, pp. 247–271. https://hal-insu.archives-ouvertes.fr/insu-00514787/document.

Guyonnet-Benaize C, Lamarche J, Masse JP, Villeneuve M, Viseur S. 2010. 3D structural modelling of small-deformations in poly-phase faults pattern. Application to the Mid-Cretaceous durance uplift, Provence (SE France). *Journal of Geodynamics* 50(2): 81–93. https://doi.org/10.1016/j.jog.2010.03.003.

Handy MR, Schmid SM, Bousquet R, Kissling E, Bernoulli D. 2010. Reconciling plate-tectonic reconstructions of Alpine Tethys with the geological-geophysical record of spreading and subduction in the Alps. *Earth-Science Reviews* 102(3-4): 121–158. https://doi.org/10.1016/j.earscirev.2010.06.002.

Hardy S, Ford M. 1997. Numerical modeling of trishear fault propagation folding and associated growth strata. *Tectonics* 16: 841–854.

Haug É. 1925. Les nappes de charriage de la Basse-Provence. Première partie – La région toulonnaise. Mémoire du Service de la Carte géologique détaillée de la France, 304 p.

Hennuy J. 2003. Sédimentation carbonatée et silicoclastique sous contôle tectonique, le bassin sud-provençal et sa plate-forme carbonatée du turonien moyen au coniacien moyen. Évolutions séquentielle, diagénétique, paléogéographique, 194 p.

Hippolyte JC, Angelier J, Bergerat F, Nury D, Guieu G. 1993. Tectonic-stratigraphic record of paleostress time changes in the Oligocene Basins of the Provence, southern France. *Tectonophysics* 226(1-4): 15–35. https://doi.org/10.1016/0040-1951(93)90108-V.

Hudec MR, Jackson MPA. 2007. Terra infirma: Understanding salt tectonics. *Earth-Science Reviews* 82(1-2): 1–28. https://doi.org/10.1016/j.earscirev.2007.01.001.

Jackson MP, Hudec MR. 2017. Salt tectonics: Principles and practice. Cambridge University Press.

Jourdan S, Bernet M, Hardwick E, Paquette JL, Tricart P, Senebier F, *et al.* 2018. Geo-thermochronology of the Saint Antonin Basin, south-eastern France. *BSGF – Earth Sciences Bulletin* 189(3). https://doi.org/10.1051/bsgf/2018013.

Labaume P, Teixell A. 2020. Evolution of salt structures of the Pyrenean rift (Chaînons Béarnais, France): From hyper-extension to tectonic inversion. *Tectonophysics* 228451. https://doi.org/10.1016/j.tecto.2020.228451.

Lacombe O, Jolivet L. 2005. Structural and kinematic relationships between Corsica and the Pyrenees-Provence domain at the time of the Pyrenean orogeny. *Tectonics* 24(1). https://doi.org/10.1029/2004TC001673.

Lacombe O, Mouthereau F. 2002. Basement-involved shortening and deep detachment tectonics in forelands of orogens: Insights from recent collision belts (Taiwan, Western Alps, Pyrenees). *Tectonics* 21(4): 1030. https://doi.org/10.1029/2001TC901018.

Lacombe O, Angelier J, Laurent P. 1992. Determining paleostress orientations from faults and calcite twins: A case study near the Sainte-Victoire Range (southern France). *Tectonophysics* 201: 141–156. https://doi.org/10.1016/0040-1951(92)90180-E.

Le Pichon X, Rangin C, Hamon Y, Loget N, Lin JY, Andreani L, *et al.* 2010. Geodynamics of the France Southeast Basin. *Bull. Soc. Geol. Fr.* 181: 477–501. https://doi.org/10.2113/gssgfbull.181.6.477.

Macchiavelli C, Vergés J, Schettino A, Fernàndez M, Turco E, Casciello E, *et al.* 2017. A new southern North Atlantic isochron map: Insights into the drift of the Iberian Plate since the Late Cretaceous. *Journal of Geophysical Research: Solid Earth* 122 (12): 9603–9626. https://doi.org/10.1002/2017JB014769.

Machhour L, Philip J. 1984. Faciès de type black-shales et laminites de l'Albien de la région de Toulon (S-E France). In: *5th European Regional Meeting of Sedimentology*, Marseille, pp. 160–261.

Machhour L, Philip J, Oudin JL. 1994. Formation of laminite deposits in anaerobic-dysaerobic marine environments. *Marine Geology* 117: 287–302.

Masse J-P. 1976. Les calcaires urgoniens de Provence. Thèse de doctorat d'État, Marseille, 445 p.

Masse J-P, Philip J. 1969. Sur la présence de brèches et de klippes sédimentaires dans l'Albien de Sainte-Anne-d'Évenos (Var). Implications paléogéographiques. *Bulletin de la Société géologique de France* XI(7): 666–669.

Masse J-P, Philip J. 1973. Mise en évidence de l'Albien au Mont Combe (Nord de Toulon, Var). Implications paléontologiques, paléogéographiques, et tectoniques. *Bulletin du BRGM, 2^{e} Série* 4: 207–214.

Masse J-P, Philip J. 1976. Paléogéographie et tectonique du Crétacé moyen en Provence. *Rev. Geogr. Phys. Geol. Dyn.* 2: 49–66.

Mauffret A, Gorini C. 1996. Structural style and geodynamic evolution of Camargue and western Provençal Basin, southeastern France. *Tectonics* 15(2): 356–375. https://doi.org/10.1029/95TC02407.

McConnell D. 1994. Fixed-hinge, basement-involved fault-propagation folds, Wyoming. *Geol. Soc. Am. Bull.* 106: 1583–1593.

Mennessier G. 1959. Étude tectonique des confins alpino-provençaux entre le Verdon et l'Argens. *Mémoires de la Société géologique de France*, XXXVIII, 4, 87: 174, VIII pl.

Mercadier C. 1984. Paléoenvironnements et sédimentologie des formations récifales du Sénonien inférieur de Sainte-Anne-d'Évenos. Massif du Gros Cerveau (Var). Thèse de Doctorat de l'Université de Provence, Marseille, 246 p.

Mitra S, Mount VS. 1998. Foreland basement-involved structures. *AAPG Bull.* 82: 70–109.

Molli G, Malavieille J. 2011. Orogenic processes and the Corsica/Apennines geodynamic evolution: Insights from {Taiwan}. *International Journal of Earth Sciences* 100(5): 1207–1224. https://doi.org/10.1007/s00531-010-0598-y.

Philip J. 1967. Modalités et importance de la transgression du Sénonien inférieur dans la région de Saint-Cyr-sur-Mer (Var). *Comptes Rendus de l'Académie des Sciences, Paris* 265: 1883–1886.

Philip J. 1970. Les formations calcaires à rudistes du Crétacé supérieur provençal et rhodanien. Thèse de doctorat d'État, Marseille, 438 p.

Philip J. 1980. Relations entre récifs à rudistes, paléostructure et tectonique synsédimentaire dans le Crétacé supérieur de la région toulonnaise (Var). In: *8e Réun. Ann. Sci. Terre*, Marseille, p. 283. Livre en dépôt à la Soc. Géol. France.

Philip J. 2012. L'exploration géologique de la Provence : deux siècles et demi de débats et de controverses. Presses des Mines, Collection Histoire Sciences et sociétés, 366 p.

Philip J, Bercovici C, Machhour L, Masse PJL. 1985. La tectonique crétacée de la région toulonnaise. In: *Réunion extraordinaire de la Société Géologique de France du 3 au 7 septembre à Marseille*. Documents du BRGM, 94, pp. 1–22.

Philip J, Masse J-P, Machhour L. 1987. L'évolution paléogéographique et structurale du front de chevauchement nord-toulonnais (Basse-Provence occidentale, France). *Bull. Soc. Géol. Fr.* 8(III): 541–550.

Rangin C, Le Pichon X, Loget N, Hamon Y, Crespy A. 2010. Gravity tectonics in the SE Basin (Provence, France) imaged with seismic data. In: Le Pichon X, Rangin C, eds. *Geodynamics of the France Southeast Basin: Importance of gravity tectonics*. Bull. Soc. géol. Fr. 181(6), pp. 503–530.

Roure F, Choukroune P. 1998. Contribution of the ECORS seismic data to the Pyrenean geology: Crustal architecture and geodynamic evolution of the Pyrenees. *Mém. Soc. géol. Fr.* 173: 37–52.

Rowan MG, Giles KA, Hearon TE, Fiduk JC. 2016. Megaflaps adjacent to salt diapirs. *AAPG Bulletin* 100(11): 1723–1747. https://doi.org/10.1306/05241616009.

Rowan MG, Urai JL, Carl Fiduk J, Kukla PA. 2019. Deformation of intrasalt competent layers in different modes of salt tectonics. *Solid Earth* 10(3): 987–1013. https://doi.org/10.5194/se-10-987-2019.

Saura E, Vergés J, Martín-Martín JD, Messager G, Moragas M, Razin P, *et al.* 2014. Syn- to post-rift diapirism and minibasins of the Central High Atlas (Morocco): The changing face of a mountain belt. *Journal of the Geological Society* 171(1): 97–105. https://doi.org/10.1144/jgs2013-079.

Saura E, Ardèvol L, Teixell A, Vergés J. 2016. Rising and falling diapirs, shifting depocenters and flap overturning in the Cretaceous Sopeira and Sant Gervàs subbasins (Ribagorça Basin, southern Pyrenees). *Tectonics*. https://doi.org/10.1002/2015TC004001.

Sibuet J-C, Srivastava SP, Spakman W. 2004. Pyrenean orogeny and plate kinematics. *Journal of Geophysical Research: Solid Earth* 109(B8). http://onlinelibrary.wiley.com/doi/10.1029/2003JB002514/full.

Soto JI, Flinch JF, Tari G, (eds.). 2017. *Permo-Triassic salt provinces of Europe, North Africa and the Atlantic Margins*. Amsterdam: Elsevier.

Stampfli GM, Borel GD. 2002. A plate tectonic model for the Paleozoic and Mesozoic constrained by dynamic plate boundaries and restored synthetic oceanic isochrons. *Earth and Planetary Science Letters* 196(1-2): 17–33. https://doi.org/10.1016/S0012-821X(01)00588-X.

Tavani S, Bertok C, Granado P, Piana F, Salas R, Vigna B, *et al.* 2018. The Iberia-Eurasia plate boundary east of the Pyrenees. *Earth-Science Reviews* 187: 314–337. https://doi.org/10.1016/j.earscirev.2018.10.008.

Tempier C. 1987. Modèle nouveau de mise en place des structures provençales. *Bulletin de la Société géologique de France* III(3): 533–540.

Ternois S, Odlum M, Ford M, Pik R, Stockli D, Tibari B, *et al.* 2019. Thermochronological Evidence of Early Orogenesis, eastern Pyrenees, France. *Tectonics* 38(4). https://doi.org/10.1029/2018TC005254.

Toucas A. 1873. Mémoire sur les terrains crétacés des environs du Beausset (Var). *Mémoires de la Société géologique de France* IX (2): 65.

Tronchetti G. 1981. Les foraminifères crétacés de Provence (Aptien-Santonien). Thèse, Marseille, 559 p.

Turco E, Macchiavelli C, Mazzoli S, Schettino A, Pierantoni PP. 2012. Kinematic evolution of Alpine Corsica in the framework of Mediterranean mountain belts. *Tectonophysics* 579: 193–206. https://doi.org/10.1016/j.tecto.2012.05.010.

Vergés J, Poprawski Y, Almar Y, Drzawiecki PA, Moragas M, Bovar-Arnal T, *et al.* 2020. Tectono-sedimentary evolution of Jurassic-Cretaceous diapiric structures: Miravete anticline, Maestrat Basin, Spain. *Basin Research*, 0–21. https://doi.org/10.1016/j.optmat.2011.11.002.

Vially R, Trémolières P. 1996. Geodynamics of the Gulf of Lion: Implications for petroleum exploration. In: *Structure and prospects of Alpine Basins and forelands*, vol. 170, Peri-Tethys Mem.

Worrall DM, Snelson S. 1989. Evolution of thenorthern Gulf of Mexico, with emphasis on Cenozoic from growth faulting and the role of salt. In: Bally AW, Palmer AR, eds. *The geology of North America – An overview*. Geological Society of America, Boulder, pp. 97–138.

Cite this article as: Wicker V, Ford M. 2021. Assessment of the tectonic role of the Triassic evaporites in the North Toulon fold-thrust belt, *BSGF - Earth Sciences Bulletin* 192: 51.